Dissertation

Development and Application of a Novel Technology for Evaluation of Personal Exposure and Online Monitoring of Environmental Aerosol Nanoparticles

THUNYAPAT THONGYEN

Division of Environmental Science and Engineering
Graduate School of Natural Science and Technology
Kanazawa University
Academic Year 2014

Dissertation

Development and Application of a Novel Technology for Evaluation of Personal Exposure and Online Monitoring of Environmental Aerosol Nanoparticles

環境エアロゾルナノ粒子個人曝露評価およびオンラインモニタリング
のための新技術の開発と応用

Graduate School of Natural Science and Technology
Kanazawa University

Major subject: Environmental Science and Engineering
Student ID No: 1123142412
Name : Thunyapat Thongyen
Chief advisor: Prof.Dr.Furuuchi Masami

Table of Contents

Chapter 1 Introduction

1.1 Aerosol Particles 1

1.2 Nanoparticle Exposure and Health Effects 2

1.3 Nanoparticles Measuring Instruments 3

1.4 Principle of Inertial Filter 4

1.5 Personal Sampler for Evaluating of Ultrafine Particles Using Inertial Filter Technology 6

1.6 Objective of Research 10

1.7 Contents of Research 10

Chapter 2 Development of $PM_{0.1}$ Personal Sampler for Evaluation of Personal Exposure to Aerosol Nanoparticles

2.1 Introduction 12

2.2 Inertial Filters and Pre-cut impactors 14

2.3 Experiments 18

2.4 Results and Discussion 23

2.5 Conclusion 29

Chapter 3 Exposure Assessment of Aerosol Nanoparticles and Chemical Compounds in Living and Working Environments

3.1 Introduction 30

3.2 Devices for Evaluation of Personal Exposure 31

3.3 Environments Discussed 34

3.4 Procedure 39

3.5 Results and Discussion 42

3.6 Conclusion 52

Chapter 4 Online Monitoring of $PM_{0.1}$ Number Concentration and Particle-bound Black Carbon Using $PM_{0.1}$ Inertial Filter

4.1 Introduction 54

4.2 $PM_{0.1}$ Separation Unit 55

4.3 Proposed Monitoring System 55
4.4 Experiments 57
4.5 Results and Discussion 59
4.6 Conclusion 63

Chapter 5 Conclusion 64
References 65
Acknowledgement 69

List of Figure Captions

Fig. 1.1 Concentration of number, surface area and volume by particle diameter.

Fig. 1.2 Exposure ratio of particles in human respiratory system.

Fig. 1.3 Single fiber collection mechanisms for fibrous filter.

Fig. 1.4 Principle of inertial filtration.

Fig. 1.5 Inertial filters for a personal nanosampler.

Fig. 1.6 Schematic of Personal Nanosampler

Fig. 1.7 Collection efficiency curves of inertial filters of PNS inlet type No.1 and No.2.

Fig. 2.1 Schematic of the main inertial filter.

Fig. 2.2 TEM grid (Glider, G600HSS)

Fig. 2.3 ATPS-20H（Shibata Scientific Technology).

Fig. 2.4 $PM_{0.1}$ personal sampler inlet and inertial filters used: (a) an outside picture and structure of $PM_{0.1}$ personal sampler inlet, (b) the pre-cut inertial filter and stainless steel (SUS) fibers used, (c) the main inertial filter (layered mesh geometry).

Fig. 2.5 Portable HARIO pump (HARIO, HSP-5000).

Fig. 2.6 Relationship between a pressure drop and flow rate of two type of portable pump; HARIO pump (HARIO, HSP-5000) for the $PM_{0.1}$ personal sampler and SKC pump for the personal nanosampler.

Fig. 2.7 Experimental setup for the inertial filter performance test.

Fig. 2.8 Measured density of generated $ZnCl_2$ particles.

Fig. 2.9 Experimental setup for the pre-cut impactors performance test.

Fig. 2.10 Dust for industrial testing No.5 (JIS No.5).

Fig. 2.11 Density of incense smoke particles.

Fig. 2.12 Nanosampler (Kanomax, Model 3180): (a) Appearance of nanosampler
(b) Structure of nanosampler.

Fig. 2.13 Collection efficiency curves for the pre-cut impactors, the pre-cut inertial filter and the main inertial filter and the combination of the pre-cut and main inertial filters.

Fig. 2.14 Effect of glue coating on TEM grids on the collection efficiency of the main inertial filter.

Fig. 2.15 Effect of glue coating on the total collection efficiency of the pre-cut and main inertial filters.

Fig. 2.16 Pressure drop with particle loading of $PM_{0.1}$ personal sampler (a) the pre-cut impactors, (b) the pre-cut inertial filter, (c) the main inertial filter, (d) the backup filter and (e) $PM_{0.1}$ personal sampler (the pre-cut impactors + the pre-cut inertial filter + the main filter + the backup filter).

Fig. 2.17 Comparison of collection efficiency of the main inertial filter before and after the particle loading of 0.1 mg.

Fig. 2.18 Comparison of aerosol particle cumulative concentrations obtained by $PM_{0.1}$ personal sampler with nanosampler.

Fig. 3.1 Schematic diagram of PNS ($PM_{0.7/0.2}$ and $_{PM0.7/0.14}$) and $PM_{0.1}$ personal sampler ($PM_{5.6/1.4/0.45/0.1}$, $PM_{4/1/0.45/0.1}$ and $PM_{2.5/1/0.45/0.1}$).

Fig. 3.2 Sampling locations for evaluation of personal exposure at sidewalk along road tunnel.

Fig. 3.3 Cigarette using dried banana leaves.

Fig. 3.4 Particle mass concentrations of collected particles at middle and mouth of tunnel, background at Kanazawa and roadside at Bangkok.

Fig. 3.5 Particle mass concentrations of collected particles at middle of tunnel, bus stop in a weekday and a weekend at Kanazawa and on road at Phnom Penh.

Fig. 3.6 Particle mass concentrations of collected particles at roadside and the breathing zone of taxi driver at Shenyang.

Fig. 3.7 article mass concentrations of collected particles at the breathing zone of train passenger in a smoking cabin.

Fig. 3.8 Particle mass concentrations of collected particles at a smoker house and the breathing zone of smoker.

Fig. 3.9 Particle mass concentrations of collected particles of a daily life in a weekday and a weekend at Phnom Penh.

Fig. 3.10 Particle mass concentrations of collected particles at the breathing zone of workers of Rubber sheet smoking (RSS): factory RSS factory-1 (September 2008) and RSS factory-2 (January 2009).

Fig. 3.11 Particle mass concentrations of collected particles at the breathing zone of workers of Rubber sheet smoking (RSS): RSS factory-3 (January2009) and RSS factory-4 (February 2009).

Fig. 3.12 Particle mass concentrations of collected particles at the breathing zone of workers of a textile factory, a print screen factory, and a TiO_2 nano-powder factory.

Fig. 3.13 Particle mass concentrations of collected particles at the breathing zone of worker of a paint factory.

Fig. 3.14 Carbon components of collected $PM_{0.1}$ particles (a) OC (b) EC and (c) OC/EC.

Fig. 3.15 Particle-bound 4-6 rings PAHs concentration at middle of tunnel and bus stop in a weekday and a weekend at Kanazawa.

Fig. 3.16 Particle-bound 4-6 rings PAHs concentration at the breathing zone of workers of Rubber sheet smoking (RSS): RSS factory-3 (January2009) and RSS factory-4 (February 2009).

Fig. 3.17 Particle-bound 4-6 rings PAHs concentration at the breathing zone of train passenger in a smoking cabin.

Fig.3.18 Particle-bound 4-6 rings PAHs concentration at the breathing zone of the breathing zone of workers of rubber sheet smoking (RSS): factory RSS factory-1 (September 2008) and RSS factory-2 (January 2009).

Fig. 3.19 BaP_{TEQ} mass fraction at middle of tunnel and bus stop in a weekday and a weekend at Kanazawa.

Fig. 3.20 BaP_{TEQ} mass fraction at the breathing zone of train passenger in a smoking cabin.

Fig.3.21 BaP_{TEQ} mass fraction at the breathing zone of workers of rubber sheet smoking (RSS): RSS factory-3 (January2009) and RSS factory-4 (February 2009).

Fig. 3.22 BaP_{TEQ} mass fraction at the breathing zone of train passenger.

Fig. 4.1 Structure of $PM_{0.1}$ separation unit.

Fig. 4.2 $PM_{0.1}$ online monitoring system proposed in the present study.

Fig. 4.3 $PM_{0.1}$ and associated BC online monitoring system proposed in the present study.

Fig. 4.4 Experimental setup for validation of $PM_{0.1}$ online monitoring system.

Fig. 4.5 $PM_{0.1}$ and associated BC online monitoring system for ambient particle monitoring.

Fig. 4.6 Number concentration of 100 nm mono-dispersed generated $ZnCl_2$ particles.

Fig. 4.7 Collection efficiency of inertial filters with pre-cut impactor filters using 100 nm mono-disperse $ZnCl_2$ particles.

Fig. 4.8 Number concentration of $PM_{0.1}$ and total particles measured by CPC and SMPS.

Fig. 4.9 $PM_{0.1}$ mass concentration of $PM_{0.1}$ measured by SMPS and $PM_{0.1}$ personal sampler.

Fig. 4.10 BC and EC mass concentration of ambient particles.

Fig. 4.11 Concentration of measured $PM_{0.1}$ particles, calculated $PM_{0.1}$ particles and measured total particles.

Chapter 1

Introduction

1.1 Aerosol Particles

Aerosol particles or particulate matter (PM) are solid matter or liquid droplets from smoke, dust, fly ash, or condensing vapors that are usually stable for least a few seconds and in some case can be suspended in the air for long time periods. The particle size is the most important parameter, which is directly linked to their potential for causing health problems. The U.S. national ambient air quality standard was originally based on particles up to 25-45 μm in size, termed total suspended particles (TSP). In 1987, EPA (United States Environmental Protection Agency) replaced the earlier TSP with an indicator that includes only those particles smaller than 10 μm, termed PM_{10}. These smaller particles cause most of the adverse health effects because of their ability to penetrate inside deeply lungs. Moreover, several recently studies indicate that significant respiratory and cardiovascular related problems, are associated with exposure to inhalable particle levels related to particle size. Particles smaller than 10 μm in diameter pose the greatest problems, because they can get deep into lungs, and some may even get into bloodstream. Exposure to such particles can affect both lungs and heart. Larger particles are of less concern, although they can irritate eyes, nose, and throat. Therefore, fine particle or $PM_{2.5}$ with a diameter less than 2.5 μm, is one-thirtieth of the diameter of a human hair (100 μm is the thickness of an average human hair), is an air pollutant that is a concern for people's health when levels in air are high. Nanoparticles or particles smaller than 0.1 μm or 100 nm ($PM_{0.1}$) are more harmful to human health because human have inadequate natural defense against $PM_{0.1}$. This is particularly important for nanoparticles (<100 nm), since a large proportion of these particles can penetrate and reach to the alveolar region (Hinds, W. C., 1999). They can also enter the cardiopulmonary system and subsequently be circulated around the human body. These particles have large surface area to volume ratios, readily allowing desorption of toxic components to human. Fig. 1.1 shows concentration of number, surface area, volume and mass by particle diameter. The two peaks of volume and mass concentration of ambient particles are around 0.5 and 10 μm respectively, while the peak of number concentration is high near 10 nm. Therefore, evaluation of particle exposure is a significant important aspect of health, especially in cases where nanoparticles are present.

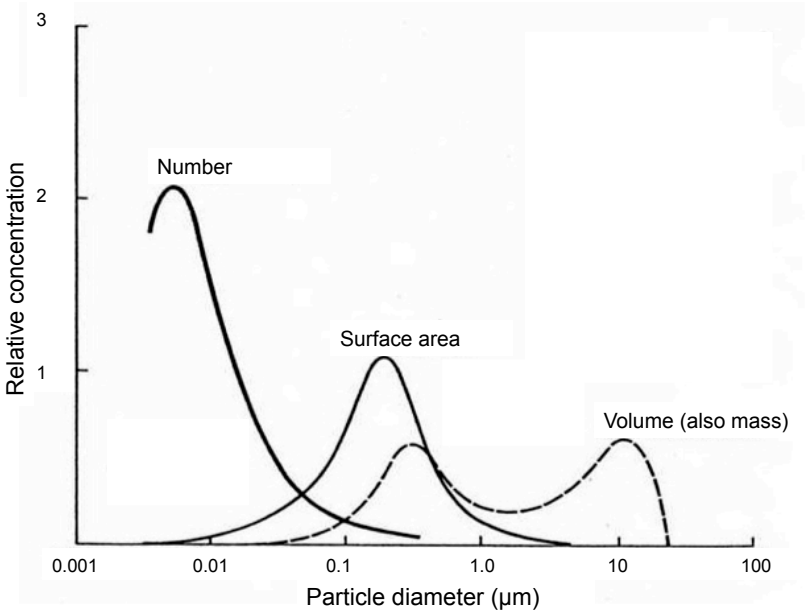

Fig. 1.1 Concentration of number, surface area and volume by particle diameter.

(Seinfeld, 1975)

1.2 Nanoparticle Exposure and Health Effects

Several scientific studies have related nanoparticle exposure to a variety of problems, including respiratory symptoms, asthma attacks, immune changes, and contributing to undesirable cardiovascular effects (Borm and Kreyling, 2004; Donaldson et al., 2002; Granum and Lovik, 2002). The effects can result in increased hospital admissions, emergency room visits, absences from school or work, and restricted activity days. People with heart or lung disease, older adults, and children are the most likely to be affected by exposure of nanoparticles, Concerning the deposition of particles in the respiratory system, exposure ratio of 1.2 m^3/hour inhalation of an adult male was shown in Fig 1.3. The nanoparticle exposure is high ratio in respiratory organs including extrathoracic region, alveolus region and also thoracic region. This is important that around 50% of nanoparticles can penetrate to alveolus region and their chemical compositions will be quickly dispersed throughout the human body (Bolch et al., 2001; Hinds, W.C., 1999; Hussain et al., 2011; Warheit, D.B., 2004).

Nanoparticles come from anthropogenic sources, e.g., volcanic eruptions, forest fire, and human activities, e.g., incinerating wastes, burning of fossil fuels and cigarette smoking. In living environments, we certainly inhale nanoparticles from surrounding sources such as vehicle exhaust and cooking using charcoal in residential area. To assess health effect, it is important to determine particle concentration and its chemical compositions. Numerous studies reported human activities, e.g., powder production in a factory, burning of agricultural

crop waste, cigarette smoking, become quiet high concentration (Behera et al., 2004; Davidson et al., 2005; Herner et al., 2005, Morawska et al., 2008; Ngo et al., 2010; Phillips and Bentley, 2001). Therefore, evaluation of nanoparticle exposure in working environments is also significant due to long-term exposure. Evaluation of nanoparticle exposure have been concerned not only nanoparticles from daily human activities and environments, but also inherent nanomaterials in a part of nanotechnological developments (Kuhlbusch et al., 2011). Although, the number of personal exposure studies in fine particles continually increased (Borgini et al., 2011; Du et al., 2010; Jahn et al., 2013; Lim et al., 2012), relatively few works have investigated personal exposure of fine particles reach to nano-size range.

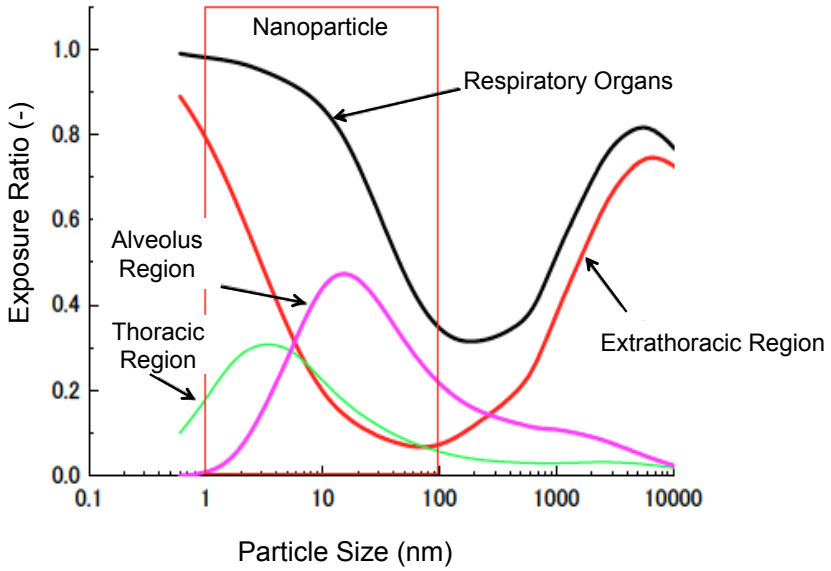

Fig. 1.2 Exposure ratio of particles in human respiratory system.

1.3 Nanoparticles Measuring Instruments

There are various techniques and instruments for detecting, measuring and characterising nanoparticles. A technique may simply detect the presence of nanoparticles, may give the quantity, the size distribution or the surface area of the nanoparticles. In recently years, nanoparticle measuring instruments have been developed during increasing knowledge of nanoparticle health effects. Instruments, which mainly carried out measurement of nanoparticles, are a condensation particle counter (CPC), a scanning mobility particle sizer (SMPS), Nanoscan SMPS, a laser particle sizer (LAS), a cascade low pressure impactor (LPI), a Nano MOUDI (Nano Micro-Orifice Uniform Deposit Impactor) and so on. The instruments can be classified to gravimetric instruments such as LPI and Nano

MOUDI, and real-time particle monitoring instruments such as CPC, SMPS, Nanoscan SMPS and LAS. CPC is used to count particle number in a total of micro- and nano-size particles, while SMPS, Nanoscan SMPS and LAS are used for measurement of particle size distribution including nanoparticle size range for number concentration and, or mass concentration. Moreover, those instruments were classified by sampling objective: a stationary samplers for particle sampling of surrounding environments or sources at a fixed location, and a portable samplers or a personal samplers with small, light and easy to carry on for mobile sampling, personal sampling and also fixed sampling locations where is inconvenient to use stationary samplers. However, there were few personal samplers applicable to nanoparticles. Example of stationary and portable samplers for nanoparticle measurement were summarized in Table 1.1

Table 1.1 Example of stationary and portable samplers for nanoparticle measurement

Stationary Sampler			
Sampler	Flow Rate	Measurement Value	Measurement Range
CPC (TSI, model 3785)	1± 0.1 L/min	Number concentration	5 nm to >3 μm
SMPS (TSI, model 3034)	1 L/min	Number and mass concentration	10~478 nm
Nanoscan SMPS (TSI, model 3910)	0.75 L/min ± 20%	Number concentration	10-420 nm
LAS (TSI, model 3340)	10-95 cm^3/min ± 5% (User-selectable)	Number concentration	90 nm to 7.5 μm
Personal Sampler			
Sampler	Flow Rate	Number of Stages	Cutpoints (range, μm)
Mini MOUDI Impactor (Model M13)	2 L/min	6, 8, 10, 13	0.01-10
Personal Nanoparticle Sampler (Tsai et al., 2012)	2 L/min	3	0.1-3.92

1.4 Principle of Inertial Filter

There are five basic mechanisms that an aerosol particle can be deposited on a fiber in a filter, interception, inertial impaction, diffusion, gravitational settling and electrostatic forces. The single-fiber efficiency is approximated as the sum of the efficiencies due to each

of the proceeding mechanisms acting individually. For collection of fine particles on the fiber, gravitational settling and electricity forces can be disregarded, since settling velocity is small with no electrostatic forces. Therefore, the fundamental of collection mechanisms of a filter are interception, inertial impaction and Brownian diffusion. Three of particle collection mechanism for fibrous filter is typically shown in Fig. 1.3. The collection efficiency depended on particle diameter and particle velocity.

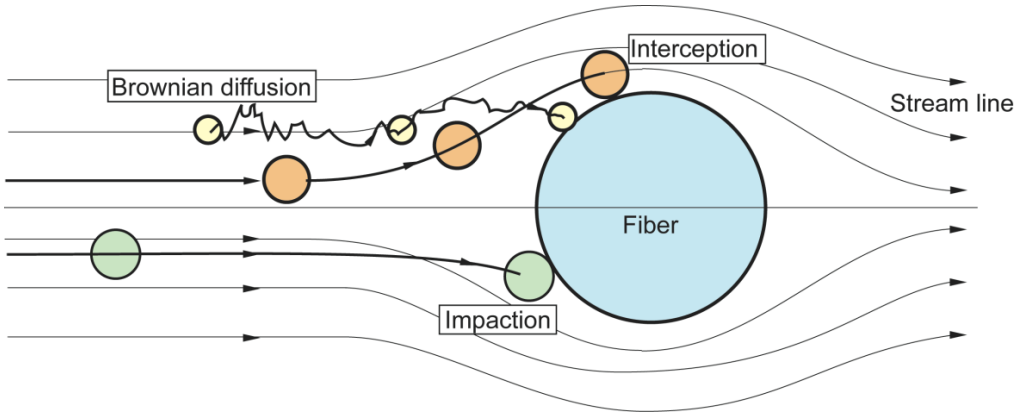

Fig. 1.3 Single fiber collection mechanisms for fibrous filter.

The inertial filter has been developed based on the inertial technology. Large particles are collected in a conventional filter by inertial impaction at a high filtration velocity while small particles are removed from air by Brownian diffusion. The parameters that involved in inertial impaction and Brownian diffusion are Stokes number (*Stk*) and Peclet number (*Pe*);

$$\mathrm{Stk} = \frac{C_c \rho_p d_p^2 u}{9 \mu d_f} \tag{1-1}$$

$$C_C = 1 + 2.514 \frac{\lambda}{d_p} + 0.80 \frac{\lambda}{d_p} \exp\left(-0.55 \frac{d_p}{\lambda} \right) \tag{1-2}$$

$$\lambda = \frac{0.0310 \left(T \right)^{1.3}}{P} \tag{1-3}$$

$$\mathrm{Pe} = \frac{u d_f}{D} \tag{1-4}$$

Where C_c is the Cunningham slip correction factor, ρ_p the particle density, d_p the particle diameter, u the filtration velocity, μ the viscosity, d_f the fiber diameter, and D the Brownian diffusivity of particles.

The collection efficiency of a filter increases with increasing *Stk* and decreasing *Pe*. Therefore, an extremely high filtration velocity and a thin fiber are capable of providing a large inertial effect.

This can change a typical collection efficiency curve with the most penetrating particle size. As denoted by the dotted curve in Fig. 1.4, the collection efficiency for larger particles increases while that for smaller particles decreases. Hence, the collection efficiency curve approaches an ideal classification of particles with dp_{50} in the nano to ultrafine range.

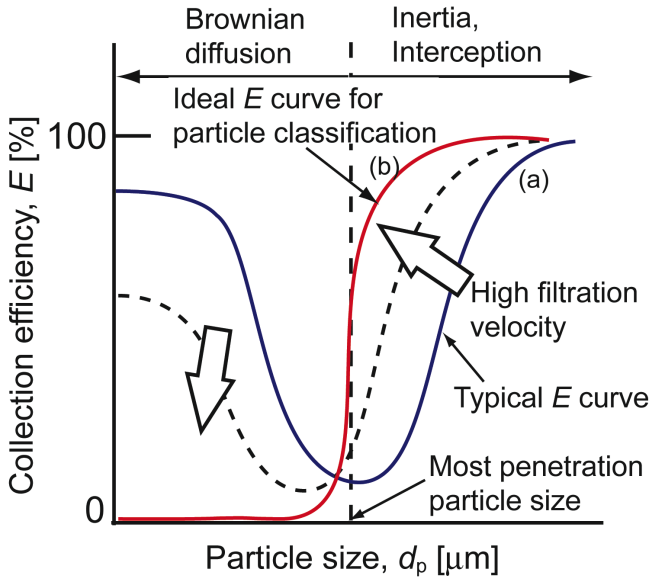

Fig. 1.4 Principle of inertial filtration.

1.5 Personal Sampler for Evaluating of Ultrafine Particles Using Inertial Filter Technology

Various types of portable personal sampler with a battery pump have been used for the evaluation of the personal exposure in workplace and living environments. However, there were few personal samplers applicable to nanoparticles because of a difficulty from a large pressure for the separation of nanoparticles using conventional methods such as the low-pressure impactor. In order to overcome this difficulty, personal nanosampler (PNS) have been developed based on the ”inertial filter” technology (Furuuchi et al., 2010).

The two-stages of inertial filters were used for the personal nanosampler. Inertial filters consisting of webbed stainless steel fibers (Nippon Seisen Co. Ltd., felt type, SUS-304) were fixed into a circular nozzle using a resin (polyoxymethylene, POM) separable cassette (Fig. 1.5). Since the web of SUS fibers has a high mechanical strength against

compression, the filter structure can be maintained at high filtration velocities, and the filtration velocity through the filter at a given pressure drop through the filter remains high. Three different diameters of SUS fiber were used, where the fiber diameter was measured through SEM photographs and shown to have a near lognormal distribution. The filter retainer on the cassette bottom was designed to hold the fiber web by 0.2 mm diameter crossed wires, in order to achieve as small a pressure drop as possible. An inertial filter cassette was employed to make handling of the sampler easier. In addition, they can be easily exchanged with new ones on site without directly touching the fibers. They can be reused after cleaning and are disposable. The specifications of the inertial filters used are summarized in Table 1.2.

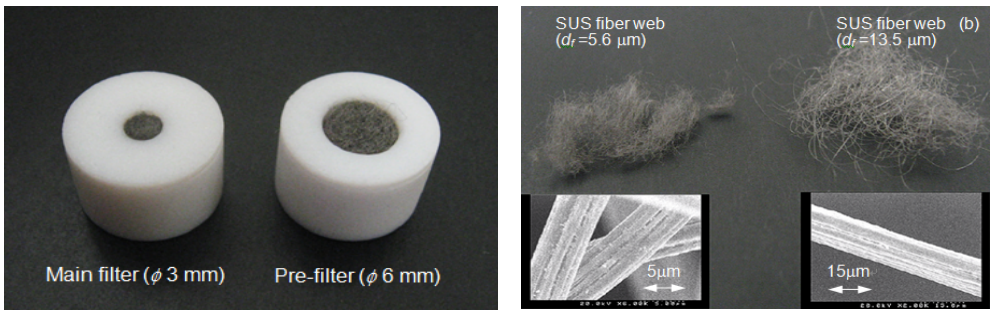

Fig. 1.5 Inertial filters for a personal nanosampler.

Table 1.2 Specification of inertial filters for the personal sampler inlet No.1 and No.2

Inlet	Inertial filter	d_f (μm)	Fiber material	Type	L_n (mm)	D_n (mm)	Q (L/min)	Fiber Loadings (mg)	Fiber volume faction α (-)	Cutoff size (field test) (nm)
No. 1	Pre	13.5 (σ_g = 1.1)	SUS-304	web	5.5	6	6	14.7–18.2	0.0143	700
	Main	9.8 (σ_g = 1.1)			4.5	3	6	3.2–3.5	0.0135	200
No. 2	Pre	9.8 (σ_g = 1.1)	SUS-304	web	5.5	6	6	20.4–22.7	0.0165	700
	Main	5.6 (σ_g = 1.1)			4.5	3	6	1.6–4.2	0.0128	140

A schematic diagram of the devised sampler, which consists of an inlet nozzle, inertial filters aligned in series, and a filter holder, is shown in Fig. 1.6. Duralumin and resin (POM) parts were used to reduce the weight of the sampler to below ~150 g. It can be clipped to a chest pocket using an inlet holder. A portable battery pump (SKC, Leland Legacy, 5−15 L/min, 1.0 kg of weight) was employed and connected to the sampler via a PVC tube. This pump was selected because it is ranked as one of the commercially available battery pumps with the largest capacity and is capable of operating 24 hrs on its internal battery.

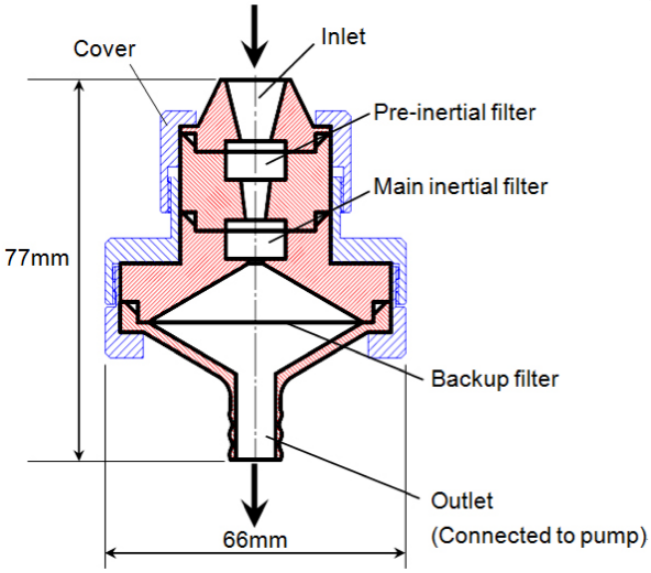

Fig. 1.6 Schematic of Personal Nanosampler.

Fig. 1.7 shows separation efficiency curves for the main inertial filter (No. 2) measured for different fiber loadings at a flow rate of 6 L/min. The collection efficiency is plotted on the basis of the aerodynamic diameter (< 300 nm) and optical diameter (> 300 nm). Solid curves were calculated from theoretical predictions in which the main collection mechanisms, inertia, diffusion and interception were taken into account, for a single fiber (Otani et al., 2007; Eryu et al., 2009). The cutoff size, or d_{p50}, decreased to ~130 nm with increasing fiber loading. This size corresponds to a Stoke's diameter of ~80 nm (Hinds, 1999) for a singly charged particle. The separation curves subsequently became steeper. For particle sizes below 30−40 nm, the collection efficiency increased slightly because of the increasing influence of diffusion (Otani et al., 2007). Separation performance is described theoretically for this condition, although the cutoff size is overestimated by 70−80%. The reason for this was not investigated in this study. However, it might be related to an effect similar to that for the aerosol dynamic lens. That is, an aerosol with a large filtration velocity may be focused after passing through each fiber. This may cause an increase in single fiber collection efficiency.

The solid curves describe tendencies. Both filter-sets provided similar separation behaviors. However, the use of a finer fiber (d_f= 5.6 μm) in the main inertial filter resulted in a smaller dp50 (~140 nm) with a steeper separation curve. The pre-filters have almost the same dp50 (~700 nm) and the separation curves are similar. The collection efficiency of particles larger than ~1 μm appears to decrease, as the result of bouncing. Hence, the inertial

filter should be used judiciously for this range of particles because of the increased risk of re-suspension or bouncing.

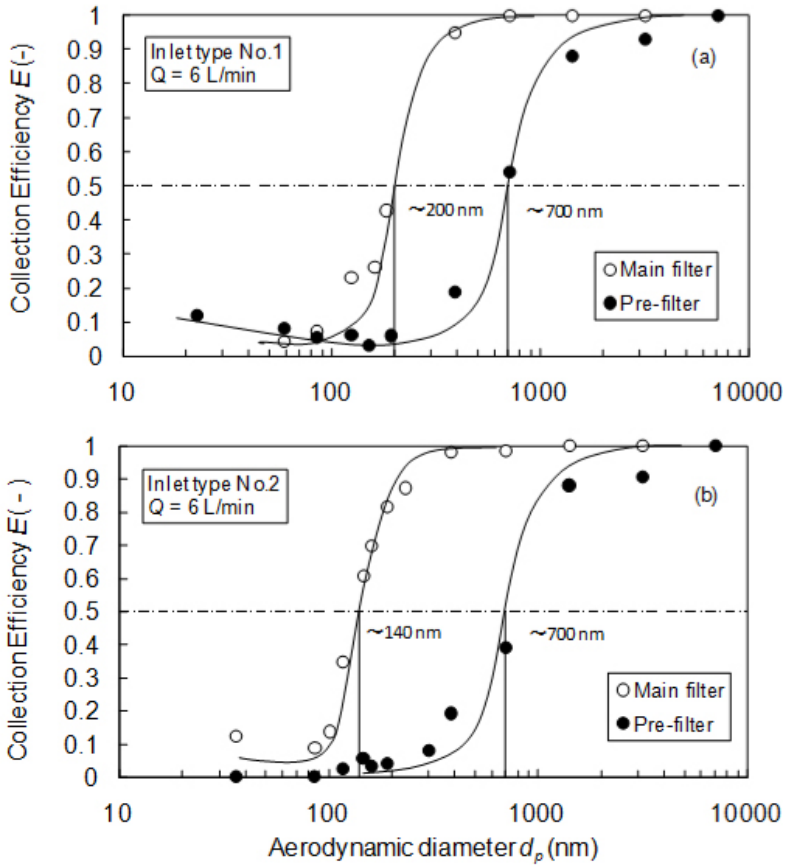

Fig. 1.7 Collection efficiency curves of inertial filters of PNS inlet type No.1 and No.2.

However, because of a difficulty in the pressure drop through the inertial filter under the limited capacity of a portable battery pump, the best achieved cutoff size was ~140 nm at 6 L/min of a sampling flow rate, which is not enough to be called as “nanoparticles”.

Although an impactor type personal sampler was recently devised for 100 nm of cutoff size (Tsai et al., 2012), its sampling flow rate (2.0 L/min) is not always enough for the chemical analysis of particles collected in working (6-8hours) and living environments (12-24 hours). Hence, the cutoff size of 100 nm should be also achieved at a practical samplng air flow rate such as 4-6 L/min or more. Another difficulty frequently encountered in the practical application is from the existence of huge and coagulated particles, which is typically observed in fine powder handling workplaces and roadside environments. The loading of these particles on the inertial filter for nanoparticle separation increases a pressure drop and also accelerates bouncing problems of coarse particles. Hence, to overcome these problems is

very important for the practical application of the personal sampler for the wide range of concentration and size distribution of particles.

1.6 Objective of Research

1. To develop and improve personal sampler for evaluation of personal exposure of $PM_{0.1}$ based on the inertial filter technology

2. To apply the developed personal sampler to evaluate personal exposure in field measurements

3. To apply the $PM_{0.1}$ inertial filter as a $PM_{0.1}$ separation unit for online monitoring system

1.7 Contents of Research

This research consists of 3 parts, which is chapter 2; Development of $PM_{0.1}$ Personal Sampler for Evaluation of Personal Exposure to Aerosol Nanoparticles, chapter 3; Exposure Assessment of Aerosol Nanoparticles and Chemical Compounds in Living and Working Environments, and chapter 4; Online Monitoring of $PM_{0.1}$ Number Concentration and Particle-bound Black Carbon Using $PM_{0.1}$ Inertial Filter.

1.7.1 Development of $PM_{0.1}$ Personal Sampler for Evaluation of Personal Exposure to Aerosol Nanoparticles

$PM_{0.1}$ personal sampler has been developed based on a new idea of a layered mesh inertial filter to evaluation of personal exposure to nanoparticles. To apply as a practical personal sampler for the evaluation of nanoparticles exposure in several environments including highly contaminated locations, pre-cut impactors were used to decrease particle load on a layered mesh inertial filter and keep it separation performance. Separation performances of the $PM_{0.1}$ personal sampler consisting of the layered mesh filter and other pre-separators were evaluated. An influence of particle loading on the pressure drop and separation performance, which is practically important, was also discussed. The $PM_{0.1}$ personal sampler was validated with a commercial instrument.

1.7.2 Exposure Assessment of Aerosol Nanoparticles and Chemical Compounds in Living and Working Environments

Personal exposure of aerosol nanoparticles at roadside and on road environments, smoking environments, exposure during daily activities and working environments were evaluated using the $PM_{0.1}$ personal sampler as the practical application. The carbon compounds of collected $PM_{0.1}$ and poly-cyclic aromatic hydrocarbons (PAHs) of collected particles were analyzed. The influences of sampling locations, human activities and environments were also discussed in relation to nanoparticle exposure and associated carbon compounds and PAHs.

1.7.3 Online Monitoring of $PM_{0.1}$ Number Concentration and Particle-bound Black Carbon Using $PM_{0.1}$ Inertial Filter

A $PM_{0.1}$ separation unit, which is based on the inertial filter technology and originally devised for the evaluation of personal exposure to nanoparticles, was applied to the online monitoring system. A condensation particle counter (CPC) was combined with the $PM_{0.1}$ separation unit for measurement of $PM_{0.1}$ number concentration. To investigate black carbon in $PM_{0.1}$, a black carbon monitor (BCM) and a multi angle absorption photometer (MAAP) were used in the online monitoring system. This is a proposal for a simple $PM_{0.1}$ monitoring tool applicable to various environments including material handling workplace and living environments.

Chapter 2

Development of $PM_{0.1}$ Personal Sampler for Evaluation of Personal Exposure to Aerosol Nanoparticles

2.1 Introduction

This chapter describes design of the $PM_{0.1}$ personal sampler, which have been developed based on a new idea of a layered mesh inertial filter to the evaluation of the personal exposure to nanoparticles. The aim of development of the $PM_{0.1}$ personal sampler is to achieve a cutoff size of 100 nm and apply as a practical personal sampler for the evaluation of nanoparticles exposure in several environments including highly contaminated locations. Therefore, separation performances of the $PM_{0.1}$ sampler consisting of a main inertial filter (a layered mesh inertial filter), a pre-cut inertial filter and pre-separators for the removal of coarser particles were evaluated. An influence of particle loading on the pressure drop and separation performance, which is practically important, was also discussed. Finally, The $PM_{0.1}$ personal sampler was validated with a conventional instrument.

To assess the health effects of airborne particulates, it is necessary to determine both the concentration and composition of the particles in the breathing zone with regards to aerodynamic particle size, which affects the regional deposition of particles inhaled into the human respiratory system. This is particularly significant important for ambient nanoparticles (<100 nm), since they can contain a large portion of hazardous chemicals from anthropogenic sources and can penetrate deeply inside lungs, eventually reach the alveolar region. Moreover, their chemical compositions will be more quickly dispersed throughout the human body (Bolch et al., 2001; Hinds, W.C., 1999; Hussain et al., 2011; Warheit, D.B., 2004). Exposure to nanoparticles has been associated with pulmonary inflammation, immune changes, and a contribution to undesirable cardiovascular effects (Borm and Kreyling, 2004; Donaldson et al., 2002; Granum and Lovik, 2002). Moreover, $PM_{0.1}$ in environments influenced by human activities, e.g., powder production in a factory, burning of agricultural crop waste, and cigarette smoking, is being reported in ever-increasing concentrations (Behera et al., 2004; Davidson et al., 2005; Herner et al., 2005, Morawska et al., 2008; Ngo et al., 2010; Phillips and Bentley, 2001). In order to evaluate health influences and risks, therefore, the monitoring of environmental nanoparticles is crucially important.

The evaluation of nanoparticle exposure has been concerned not only on nanoparticles from daily human activities and environments, but also on nanomaterials that are an inherent

part of nanotechnological developments (Kuhlbusch et al., 2011). Although the number of personal exposure studies on fine particles has continually increased (Borgini et al., 2011; Du et al., 2010; Jahn et al., 2013; Lim et al., 2012), relatively few studies have focused on monitoring the personal exposure to fine particles in the nano-size range via a portable personal sampler (Young et al., 2013). Therefore, the development of a portable personal sampler that could be used to evaluate nanoparticle exposure would be indispensable in any discussion on the health risks and influences posed by nanoparticles.

Various types of portable personal samplers equipped with a battery pump have been used for the evaluation of the personal exposure in workplaces and in living environments. Few of these personal samplers, however, have been applicable to the collection of nanoparticles. This has been due to the difficulty posed by the large degree of pressure drop that is needed for the separation of nanoparticles when using conventional methods that employ a low-pressure impactor. In order to overcome this difficulty, the authors developed a personal sampler based on the "inertial filter" technology (Furuuchi et al., 2010). However, because of the difficulty posed by a pressure drop through the inertial filter under the limited capacity of a portable battery pump, the best cutoff size that could achieved was ~140 nm with a 6 L/min of a sampling flow rate, which was insufficient for a characterization as "nanoparticles". Although an impactor type of personal sampler was recently devised with a cutoff size of 100 nm (Tsai et al., 2012), its sampling flow rate (2.0 L/min), was not always sufficient for the chemical analysis of particles that could be collected in working (6-8hours) and living environments (12-24 hours). Hence, a cutoff size of 100 nm must be achieved for a practical sampling air-flow rate that should approximate 4-6 L/min, or more. Another difficulty frequently encountered in the practical application comes from the existence of huge and coagulated particles, which are typically observed in the handling of fine powder in workplaces and in the vicinity of roadside environments. The loading of these particles on the inertial filter for nanoparticle separation increases the pressure drop and also accelerates the rate of bouncing problems encountered with coarse particles. Hence, given the wide range of concentration and size distribution of particles, it is very important to overcome these problems if the practical application of a personal sampler is to be effective.

In this study, the $PM_{0.1}$ sampler for the evaluation of the personal exposure to nanoparticles was designed based on a novel approach that uses a layered mesh inertial filter while targeting the application to practical environments including roadsides and highly contaminated workplaces. Separation performances were evaluated for the $PM_{0.1}$ sampler consisting of the layered mesh filter and other pre-separators for the removal of coarse

particles. The influence of particle loading on the pressure drop and separation performance, which is important for practical applications, was also evaluated.

2.2 Inertial Filters and Pre-cut Impactors

2.2.1 Layered Mesh Inertial Filter for $PM_{0.1}$ Separation

The structure of a layered mesh inertial filter, which is for the separation of $PM_{0.1}$ and refered as the main inertial filter was shown in Fig. 2.1. The layered mesh inertial filter consists of layered square mesh copper TEM grids (Fig. 2.2) commercially available (Glider, G600HSS) sandwiched by manufactured copper spacers with circular hole (Ø 1.9 mm, t = 30 μm) stacked in a circular nozzle (Ø 3 mm, 9 mm nozzle length) with a bell shaped inlet through an aluminum cartridge. Comparing to the geometry of an original inertial filter using webbed stainless steel fibers (Otani et al., 2007; Eryu, K. et al., 2009; Furuuchi et al., 2010), the layered TEM grids can easily provide a uniform structure of fibers aligned perpendicular to the flow direction along the nozzle, which may maximize the inertial effect on particles and provide a less pressure drop for the same separation performance. A key point of the layered-mesh is uniformity structure to project the flow direction in the preparation of the layered-mesh inertial filter since the aerosol particles may penetrate directly through open spots of the area covered by mesh wires because of a large inertial effect (Eryu, K. et al., 2009). Hence, wire mesh screens have to be aligned tangentially uniform in order to maximize the coverage of the nozzle cross section by mesh wires. The advantages of the layered mesh inertial filter cannot be obtained by the original structure of randomly orientated SUS fibers packed in a circular nozzle since it is difficult to make the structure of packed fibers uniform over the cross section and depth of a small diameter of nozzle less than 2 millimeters. Particles collected on the layered mesh inertial filter can be analyzed its chemical components such as PAHs by the extraction, e.g., immersing TEM grids in a solution for the extraction. Specifications of the TEM grid are listed in Table 2.1. The number of TEM grids and spacers were decided as 5 for each based on the preliminary experiments and numerical analysis (Eryu, K. et al., 2009; Takebayashi, 2011).

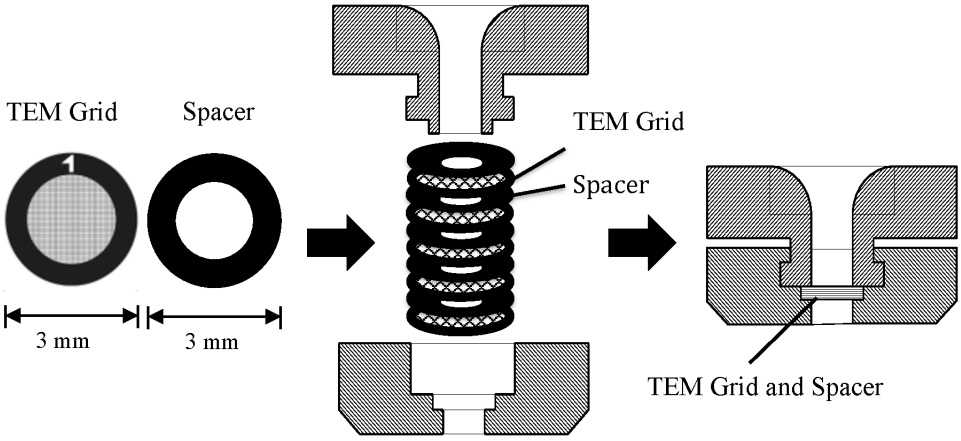

Fig. 2.1 Schematic of the main inertial filter.

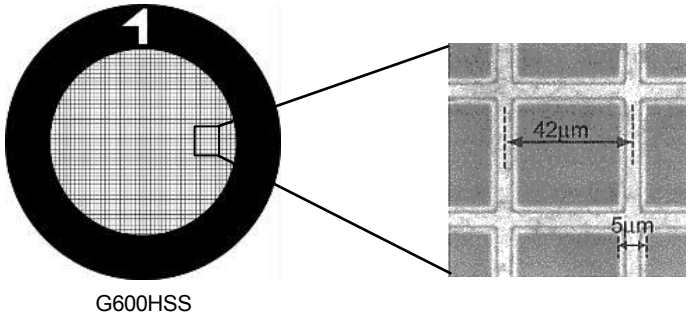

Fig. 2.2 TEM grid (Glider, G600HSS).

Table 2.1 Specification of TEM grids used for the layered mesh inertial filter

Grid type	Code	Material	Mesh (lines/inch)	Pitch (μm)	Bar width (μm)	Hole width (μm)	Thickness (μm)	Q (L/min)	Cutoff size (nm)
square mesh	Glider G600HSS	Cu	600	42	5	37	8	5	100

2.2.2 Pre-cut Inertial Filter for $PM_{0.5}$

In order to prevent clogging and bouncing of coarse particles on the layered mesh $PM_{0.1}$ inertial filter, a pre-cut inertial filter consisting of webbed SUS fibers (d_f=9.8 μm) packed in a Ø 4.75 mm circular nozzle (5.5 mm length) through a metal cartridge was used upstream the layered mesh inertial filter. This type of the inertial filter has a relatively large dust loading capacity and can provide a less pressure drop than that of the impactor. The pre-cut inertial filter has the same geometry with the original one but different diameter of nozzle and SUS-fiber loading were used to decrease the cutoff size from 700 nm to 450 nm. This

may reduce the amount of particles penetrating to the layered mesh inertial filter to keep its performance. Specification of the pre-cut inertial filter is shown in Table 2.2.

Table 2.2 Specification of the pre-cut inertial filter

Inertial Filter	d_f (μm)	Fiber material	Type	L_n (mm)	D_n (mm)	Q (L/min)	Fiber loadings (mg)	Fiber volume fraction (-)	Cutoff size (nm)
Pre-cut inertial filter	9.8	SUS-316L	web	5.5	4.75	5	10	0.0133	450

2.2.3 Pre-cut Impactors

Although the pre-cut inertial filter is expected to have a larger capacity of particle loading and a less re-suspended particles comparing with an impaction plate of the impactor, a dust loading capacity was suspected to be not enough for the measurement in highly contaminated environments by huge and coagulated particles, which are typically observed in fine powder handling processes and road side environments. In order to avoid these particles to penetrate into the pre-cut and layered mesh inertial filters, therefore, a commercially available two stage pre-cut impactors (SHIBATA, ATPS-20H) was used for the removal of particles in the micron size range. Appearance of ATPH-20H was shown in Fig. 2.3. Cutoff sizes of 1st and 2nd stage of the pre-cut impcators are estimated by an equation for inertial separation (Hinds, W.C., 1999) respectively as 5.6 and 1.4 μm at 5 L/min, which are originally designed as 10 and 2.5 μm at 1.5 L/min. The pre-cut impactors are practically important in workplaces highly contaminated by coagulated particles in order to keep the separation performance of the inertial filters and to minimize the pressure drop due to the particle loading

Fig. 2.3 ATPS-20H（Shibata Scientific Technology).

2.2.4 $PM_{0.1}$ Inlet for a Personal Sampler

Fig. 2.4 shows the geometry of the $PM_{0.1}$ personal sampler inlet, which consists of above two different types of inertial filters located downstream the two stage pre-cut impactors and followed by a backup filter on a thin stainless filter holder. The surface of an impaction plate of 1st stage of the pre-cut impactor was covered by silicon grease (Dow Corning, 03253589) to a uniform thickness around 0.2 mm while a 10 mm diameter of glass fiber filter (Pallflex, T60A20) was attached on an impaction plate of 2nd stage. The outlet of the $PM_{0.1}$ personal sampler was connected to a portable battery pump (Hario Sci., HSP-5000) (Fig. 2.5) with a flexible resin tube. Weight of the $PM_{0.1}$ personal sampler is 112 g of sampler inlet (6.5 cm maximum width and 11.4 cm height) and 700 g of the portable pump (85 mm width, 60 mm depth and 155 mm height) can be acceptable for handle sampler.

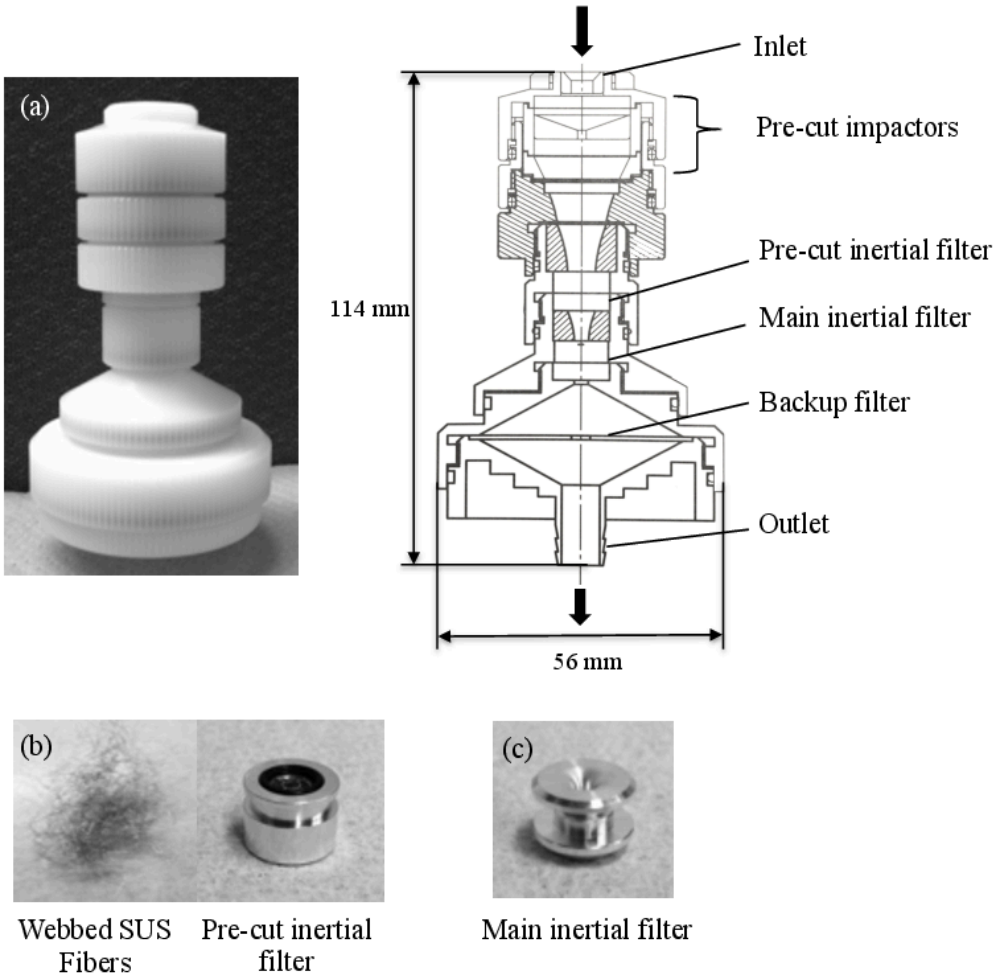

Fig. 2.4 $PM_{0.1}$ personal sampler inlet and inertial filters used: (a) an outside picture and structure of $PM_{0.1}$ personal sampler inlet, (b) the pre-cut inertial filter and stainless steel (SUS) fibers used, (c) the main inertial filter (layered mesh geometry).

Fig. 2.5 Portable HARIO pump（HARIO, HSP-5000).

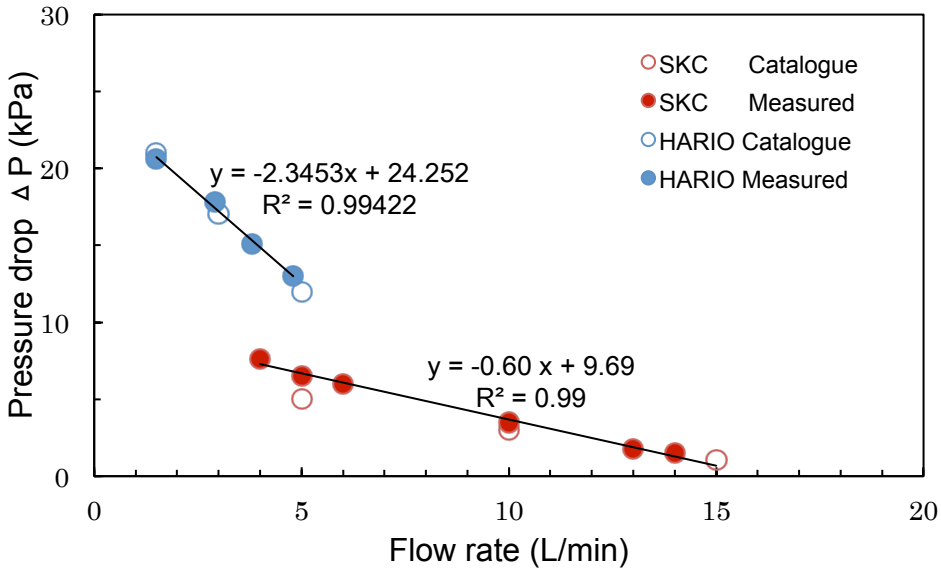

Fig. 2.6 Relationship between a pressure drop and flow rate of two type of portable pump; HARIO pump (HARIO, HSP-5000) for the $PM_{0.1}$ personal sampler and SKC pump for the personal nanosampler.

2.3 Experiments

2.3.1 Separation performances of inertial filters and pre-cut impactors

The separation performance of the inertial filters was evaluated by an experimental setup shown in Fig. 2.7, which consists of an evaporation-condensation type aerosol generator, a nitrogen gas generator for carrier gas supply, HEPA Filters, mass flow controllers, a neutralizer (^{241}Am), a differential mobility analyzer (DMA), a test inertial filter in a holder, a digital manometer and measuring instruments for particle number

concentration. The performance was evaluated following a reported procedure (Furuuchi, M et al., 2010). $ZnCl_2$ powder was dosed on an alumina boat in a tubular image furnace, where $ZnCl_2$ was heated up to 190-320 °C then cooled to a room temperature to obtain $ZnCl_2$ particles. After classifying generated particles by DMA, aerosol particles were used as the test aerosol. The mono-dispersed $ZnCl_2$ particles were diluted with air through a HEPA filter and supplied to the inertial filter put in a holder.

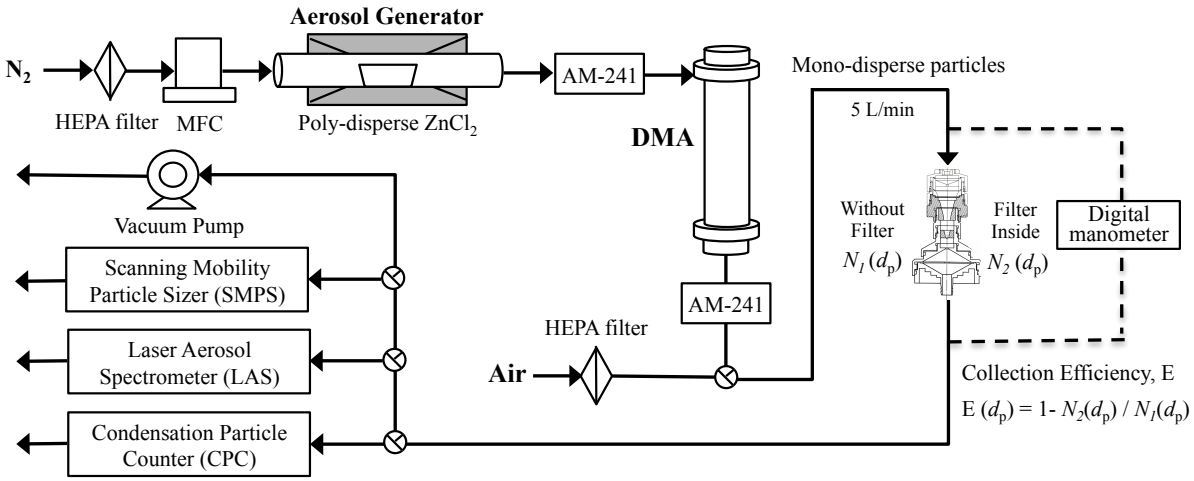

Fig. 2.7 Experimental setup for the inertial filter performance test.

The collection efficiency was determined based on the number concentration measured by a laser aerosol spectrometer (TSI, LAS model 3340), a condensation particle counter (TSI, CPC model 3785) and a scanning mobility particle sizer (TSI, SMPS model 3080). A pressure drop through the inertial filter was monitored using a digital manometer (EXTECH, HD 750). The mobility equivalent diameter of $ZnCl_2$ particles was converted to the aerodynamic diameter using a measured density (1508 kg/m^3 averaged for 40 nm to 350 nm) of generated particles using an aerosol particle mass analyzer (KANOMAX, APM model 3600). The density of generated $ZnCl_2$ particles was shown in Fig. 2.8

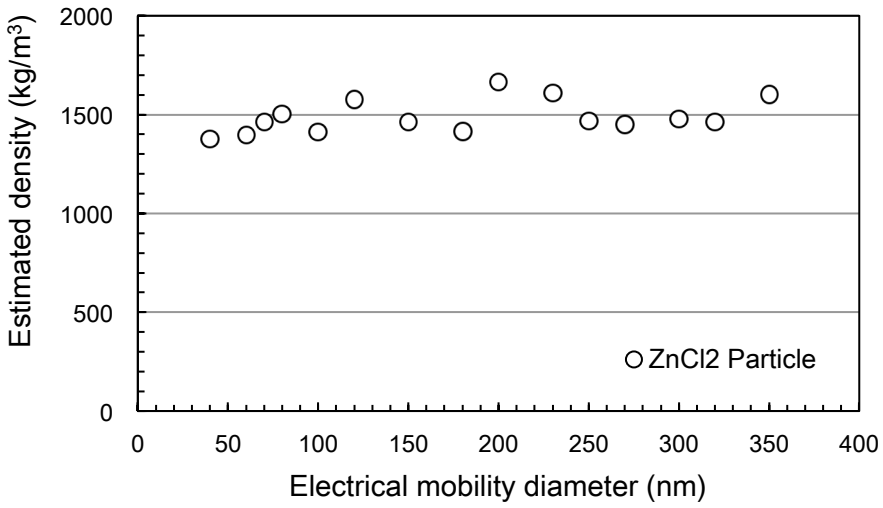

Fig. 2.8 Measured density of generated $ZnCl_2$ particles.

The performance of pre-cut impactors was evaluated using a configuration shown in Fig. 2.9. A condensation aerosol generator (TOPAS, SLG 270) was used to obtain a large number concentration of mono-dispersed NaCl coarse particles, which are electrically neutral. Generated mono-disperse NaCl particles were diluted by mixing with filtered air by a HEPA filter and supplied to the pre-cut impactor filters. The collection efficiency of pre-cut impactor filters was determined based on the number concentration measured by an aerosol particle sizer (TSI, APS model 3321). A pressure drop through the inertial filter was also monitored using a digital manometer (EXTECH, HD 750).

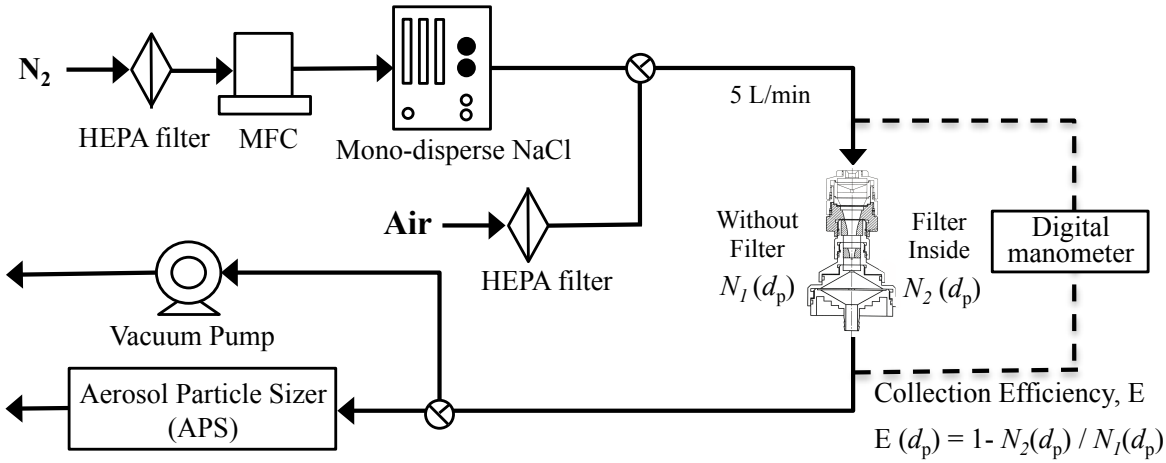

Fig. 2.9 Experimental setup for the pre-cut impactors performance test.

2.3.2 Effect of fiber coating of inertial filters

An influence of a surface treatment of inertial filter fibers to reduce a bouncing effect of coarse particles was also investigated. Fiber surfaces of the pre-cut and the main inertial filters were coated by glue, or, by dropping 1 wt% water solution of water soluble glue (Tombo, HCA-122) onto the pre-cut and main inertial filters held on the PNS inlet then drying by flowing a HEPA filtered air through each inertial filter for 1 hour. From the observation by an optical microscope, there was no remaining water glue solution or dried glue at any corners and edges of mesh grids, which may influence the flow and particle motion.

2.3.3 Influence of particle loading on pressure drop

Influences of particle loading on the pressure drop and separation performance of the PNS inlet were investigated for different size range of particles: coarse particles in micron order which may be predominant in some workplaces or roadside and fine particles which are main fraction of smoke particles including cigarette smoke and automobile exhaust particles etc. As loading test dusts, JIS No.5 as shown in Fig. 2.10, mineral dust and 85±5% of which is in > 5 μm in mass basis, was used as coarse particles. The chemical compositions of JIS No.5 are SiO_2 > 45% mass and Al_2O_3 > 20% mass. Particle size distribution of JIS No.5 was shown in Table 2.3. Density of JIS No.5 is more than 1950 kg/m^3. As fine loading test particles, incense smoke particles, which are of prominent concentration in a range between 100-200 nm, were used. The JIS No.5 dust was dispersed by an ejector (Sympatec, RODOS type) to a mixing box then introduced to the PNS. Incense smoke particles with 1950 kg/m^3 of average measured density from 40 nm to 350 nm (Fig. 2.11), were diluted by filtered air through a HEPA filter then introduced at to the PNS after. In order to obtain various particle loadings on the filters, the sampling was adjusted between 60 to 120 min for JIS No.5 dust and between 5 to 10 min for incense smoke particles. Pressure drop was measured by a digital manometer (EXTECH, HD 750) before and after sampling.

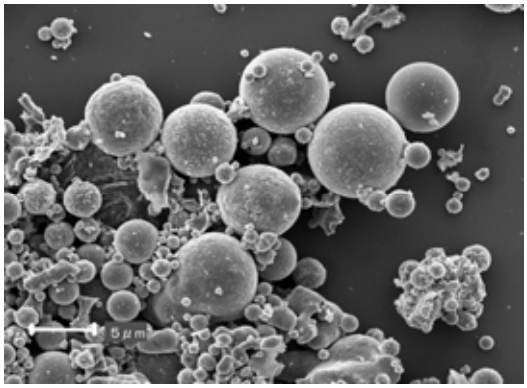

Fig. 2.10 Dust for industrial testing No.5 (JIS No.5).

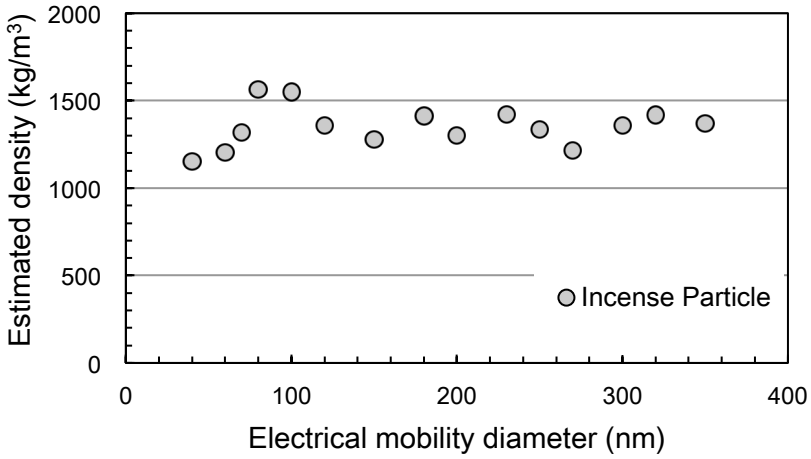

Fig. 2.11 Density of incense smoke particles.

Table 2.3 Particle size distribution of JIS No.5 (particle size and oversize on mass base)

Particle Size	Oversize (on Mass Base), %
5 μm	84 ± 5 %
10 μm	60 ± 3 %
20 μm	32 ± 3 %
30 μm	15 ± 3 %
45 μm	8 ± 3 %
105 μm	0%

2.3.4 Validation of $PM_{0.1}$ personal sampler

For the validation of measurement by the $PM_{0.1}$ personal sampler, the concentration and size distribution of ambient aerosol particles were compared between those by the $PM_{0.1}$ personal sampler and the Nanosampler as shown in Fig. 2.12 (NS, KANOMAX, Model 3180; Furuuchi *et al*., 2010) after the same period of aerosol sampling. The validation has been conducted at a balcony on 6th floor of a 7-story building of Kanazawa University in Kakuma campus, Kanazawa. Binder-less quartz fibrous filters (Pallflex, 2500QAT- UP) were used for the validation, where they were weighed after the conditioning at 20°C and 50% RH in a weighing chamber for 48 hours both before and after the sampling.

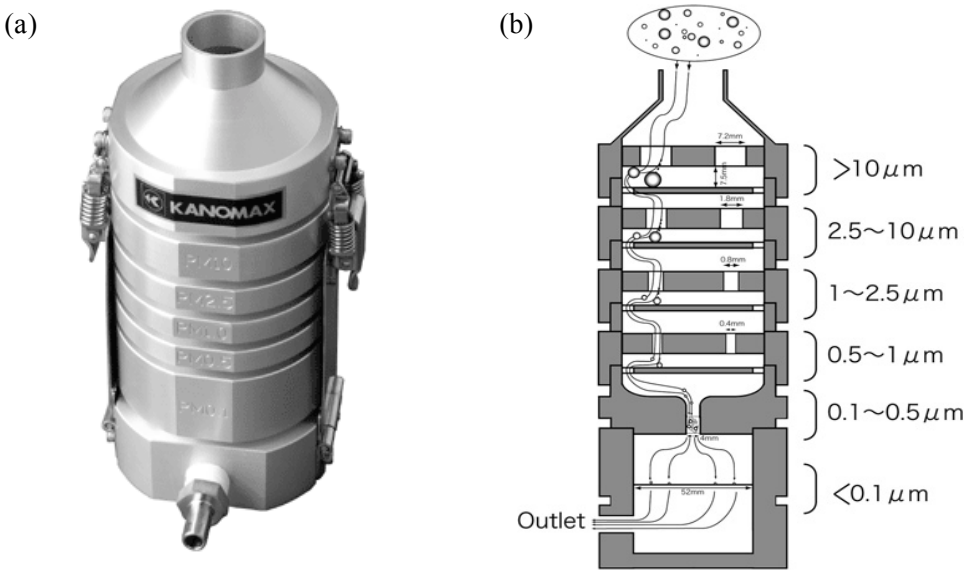

Fig. 2.12 Nanosampler (Kanomax, Model 3180): (a) Appearance of nanosampler (b) Structure of nanosampler.

2.4 Results and Discussion

2.4.1 Separation performance of the inertial filters

Fig. 2.13 shows collection efficiency curves for the pre-cut and main inertial filter along with the combination of those filters and the pre-cut impactors measured at 5 L/min of air flow rate. The cutoff size of the pre-cut filter was estimated as ~ 450 nm at a pressure drop of 0.6 kPa. The cutoff size of the main filter could be adjusted as ~ 100 nm by changing the filtration velocity, or, size of a spacer hole, with an acceptable steepness of the efficiency curve at 4.6 kPa of pressure drop. A dashed curve in Fig.2.12 denotes a precitition based on the filtration theory along with numerical simulation for a fiber with square cross-section

(Hinds, 1999; Otani et al., 2007; Eryu et al., 2009), where fiber volume fraction *a* was ajusted to fit as being d_{p50} = 100 nm (a = 0.21). Although there is a good consistency in the separation tendency between measured and precited efficiencies, the measured collection efficiency for coarse particles larger than ~ 200 nm is slightly lower than that from the prediction. This may be from influences of bouncing or re-suspension on TEM gird mesh fibers in this size range of particles. Because of Brownian diffusion, the collection efficiency for 10-20 nm of particles increased both in the pre-cut inertial filter and the main inertial filter. This may increase more for particles for smaller than 10 nm but in the particle mass point of view, it may not be so important. The pre-cut inertial filter just has a slight influence on the main filter performance. 5.2 and 7.7 kPa of the total pressure drop through respectively for tandem inertial filters and tandem inertial filters + pre-cut impactors + a backup filter are low enough to be operated by a portable battery pump (the maximum allowable pressure drop is 15 kPa at 5 L/min) of. This leads to a large allowance for an increase in pressure drop due to particle loading and tubing.

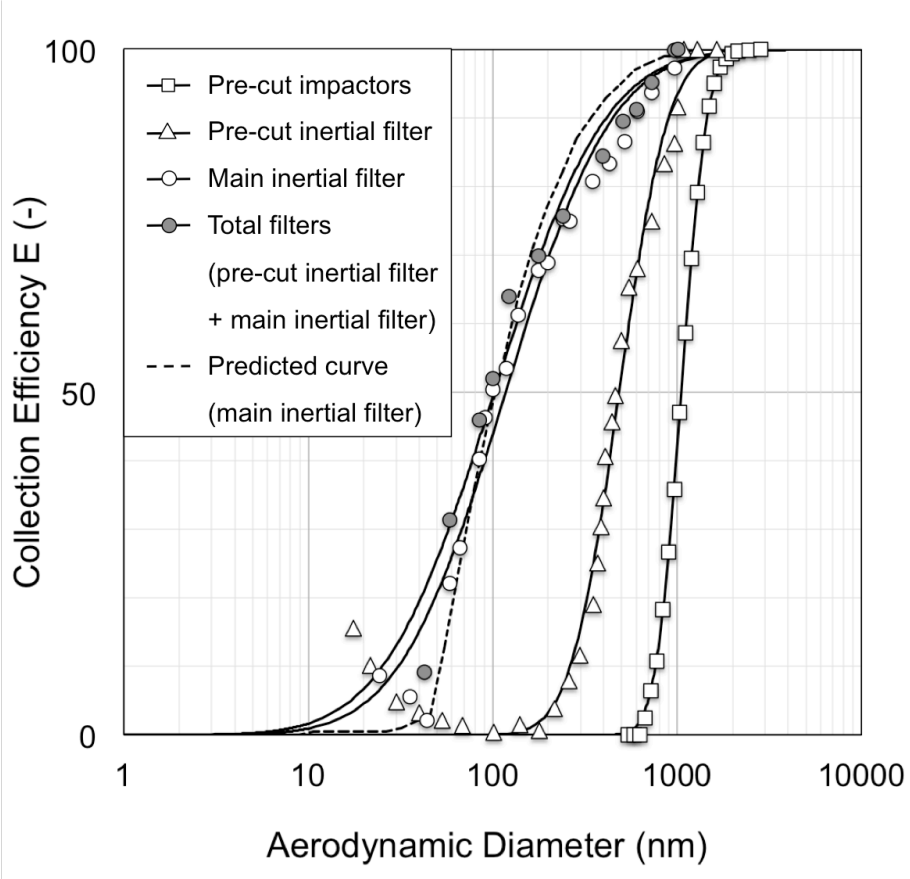

Fig. 2.13 Collection efficiency curves for the pre-cut impactors, the pre-cut inertial filter and the main inertial filter and the combination of the pre-cut and main inertial filters.

As shown in Fig. 2.14, the collection efficiency of the main inertial filter was clearly improved for coarse particles larger than ~ 200 nm by glue coating and almost reached to the predicted value, or, the maximum performance, denoted by a dashed curve. Fig. 2.15 shows total collection efficiency curves for the glue coated pre- and main inertial filters. An increase in the collection efficiency is negligibly small for the pre-inertial filter so that an improvement in the performance mostly corresponds to that in the main inertial filter. The pressure drop through of glued inertial filters increased for 10~20%, corresponding to the total pressure drop through two inertial filters of 8.10 kPa, which is still much lower than the allowable ones (15 kPa). Hence, the coating by water-soluble glue can be a tool to improve the separation performance of coarse particles although a back ground for chemical analysis of particles collected on TEM grids should be carefully evaluated.

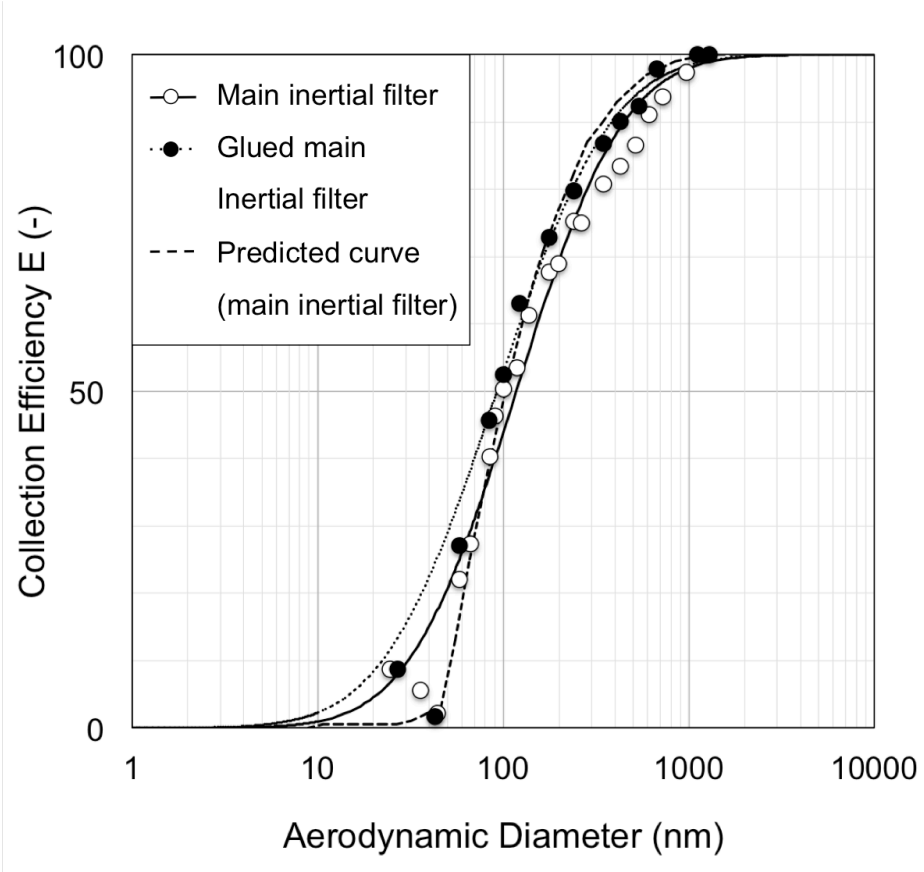

Fig. 2.14 Effect of glue coating on TEM grids on the collection efficiency of the main inertial filter.

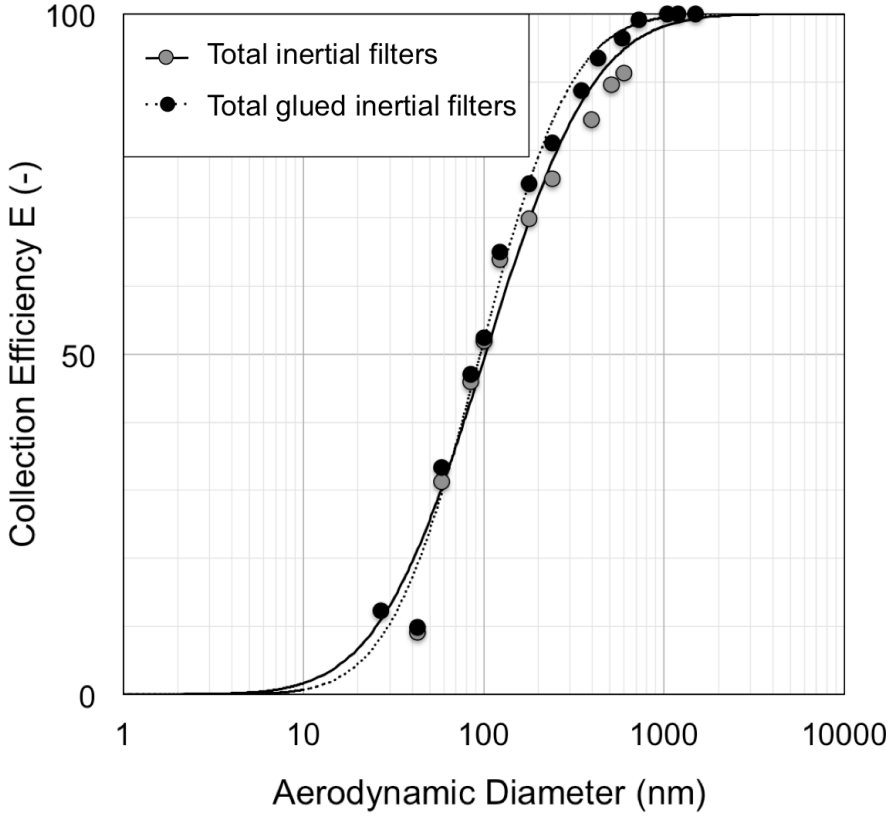

Fig. 2.15 Effect of glue coating on the total collection efficiency of the pre-cut and main inertial filters.

2.4.2 Influence of particle loading on pressure drop and separation performance

Total pressure drops through the pre-cut impactors, the inertial filters and the backup filter of $PM_{0.1}$ personal sampler are shown respectively in Figs. 2.16 (a)-(d) along with that of the total $PM_{0.1}$ personal sampler (Fig. 2.16 (e)) in relation to loaded masses of JIS No.5 test dust and incense particles. The total pressure drop was increased by dust loading up to the maximum allowance pressure, or, 15 kPa of the portable battery pump. A predominant increase in the pressure drop is in the main inertial filter especially for the incense particles while those in impactors, the pre-filter and a backup filter is not so important. Depending on size and characteristics of particles, the maximum amount of particles collected on the backup filter, which should be used not only for mass evaluation but also for various chemical analysis, may range between 0.1 ~ 0.3 mg for the present battery pump. This amount is sufficient to analysis of chemicals such as carbon components and polycyclic aromatic hydrocarbons (PAHs) and it can be increased by a pump with a larger capacity.

The separation performance of the main inertial filter with 0.1 mg of loaded incense particles, which corresponds to the maximum loading in the present case, was evaluated. A collection efficiency curve for the main inertial filter with 0.1 mg loading is shown in Fig.2.18. The cutoff size was decreased to ~ 94 nm, or, ~ 6 % to that of the non-loaded case. This may be practically acceptable in many of field measurements.

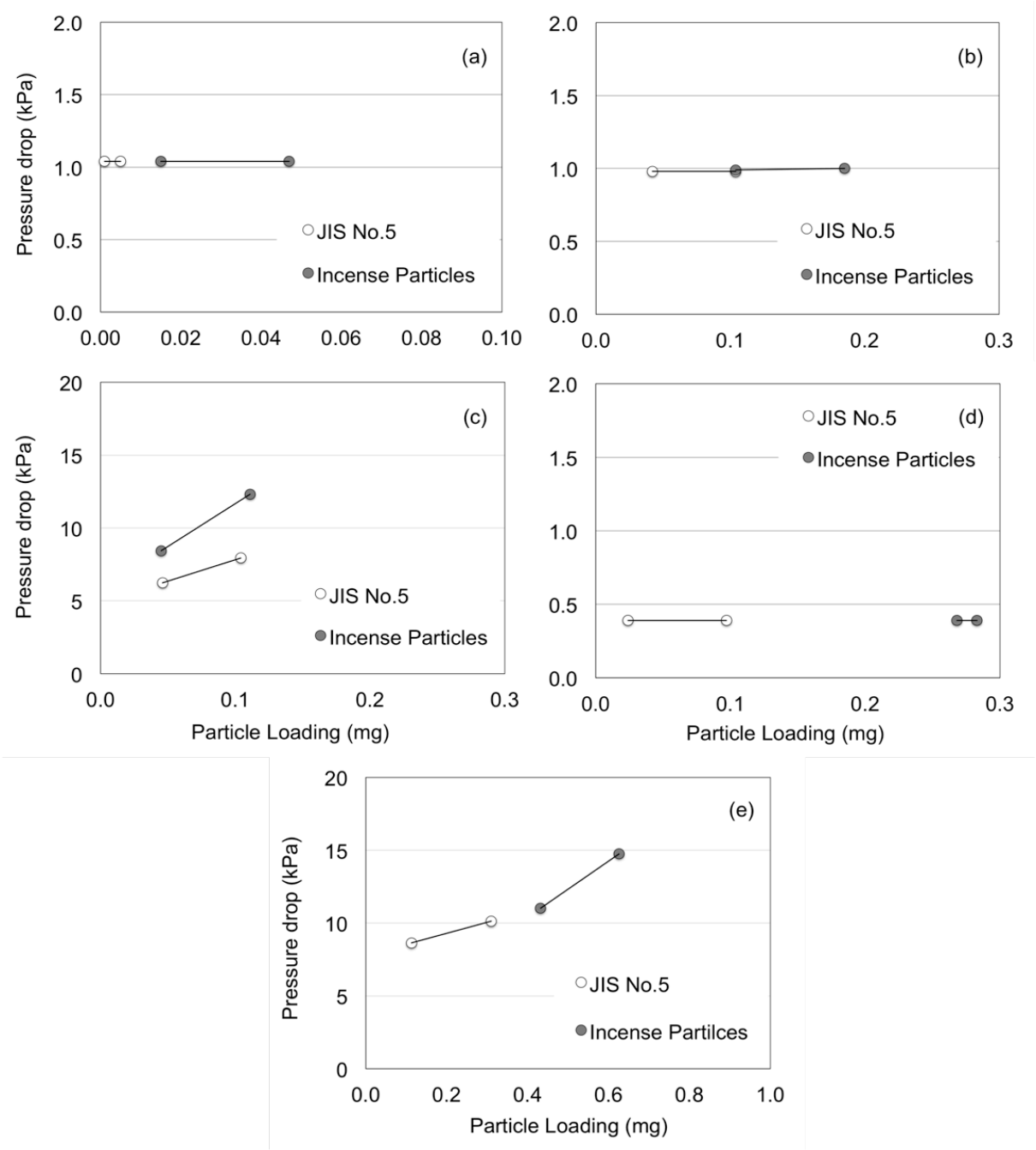

Fig. 2.16 Pressure drop with particle loading of $PM_{0.1}$ personal sampler (a) the pre-cut impactors, (b) the pre-cut inertial filter, (c) the main inertial filter, (d) the backup filter and (e) $PM_{0.1}$ personal sampler (the pre-cut impactors + the pre-cut inertial filter + the main filter + the backup filter).

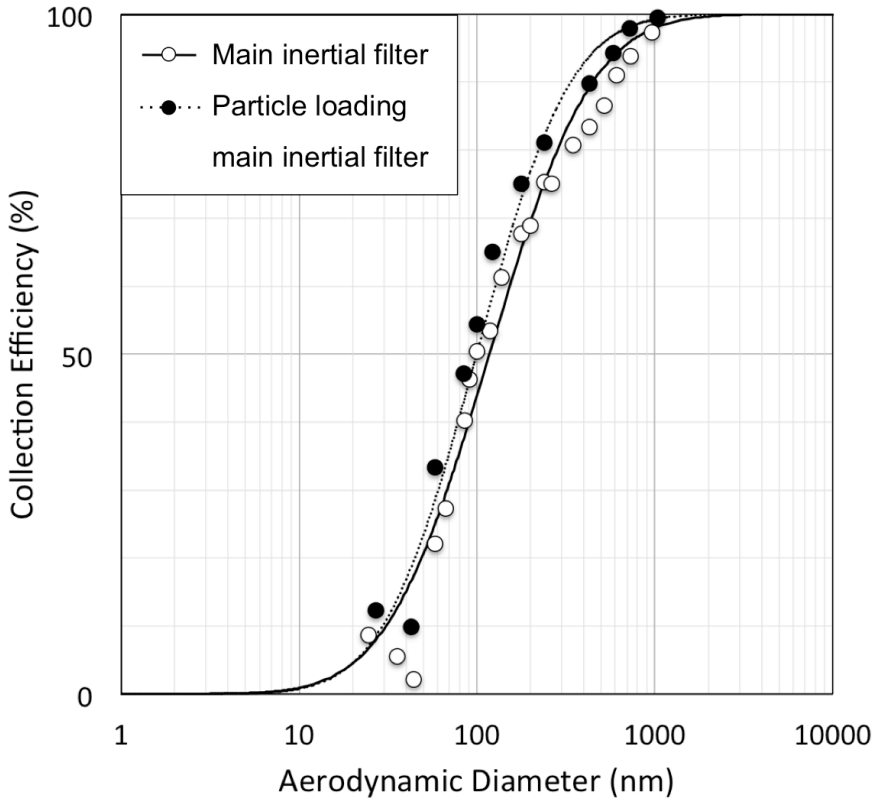

Fig. 2.17 Comparison of collection efficiency of the main inertial filter before and after the particle loading of 0.1 mg.

2.4.3 Validation of $PM_{0.1}$ personal sampler with Nanosampler

Fig. 2.18 shows the cumulative concentration of size-fractionated particles collected by the $PM_{0.1}$ personal sampler with pre-cut impactors compared with that by the Nanosampler (Kanomax, Model 3180) (Furuuchi *et al*., 2011). Similarity of the concentration and size distribution between those from PNS and NS are reasonable.

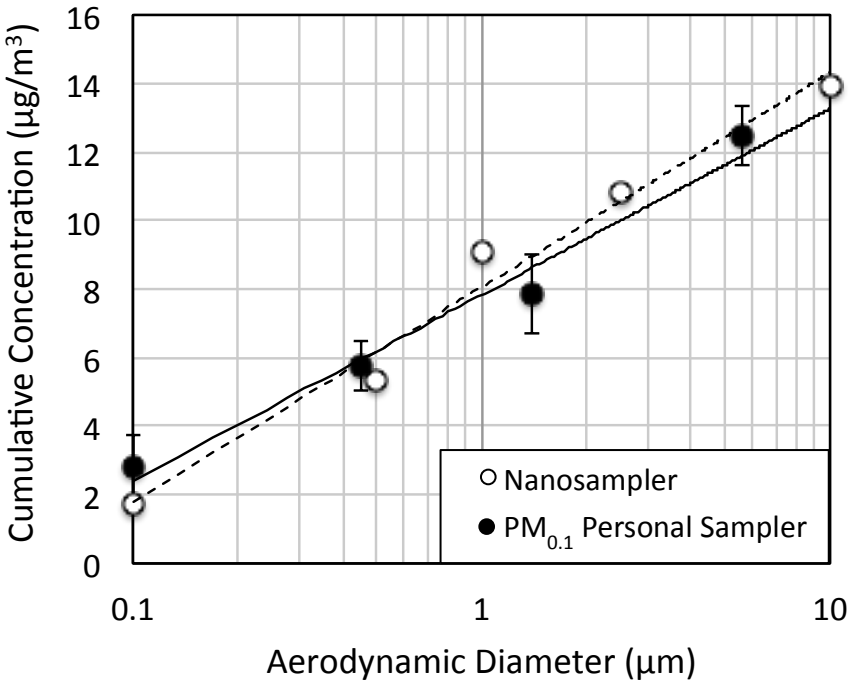

Fig. 2.18 Comparison of aerosol particle cumulative concentrations obtained by $PM_{0.1}$ personal sampler with Nanosampler.

2.5 Conclusion

For practical applications in environments that include sampling from roadsides and in highly contaminated workplaces, the $PM_{0.1}$ personal sampler was successfully devised by improving a prototype of the personal sampler for the evaluation of personal exposure to nanoparticles (Furuuchi et al., 2010). The inertial filter with a layered mesh geometry demonstrated a separation performance with a cutoff size of 100 nm and a small pressure drop of ~5 kPa. Through the combination of a layered mesh inertial filter for the $PM_{0.1}$ and pre-cut impactors for the removal of huge or coagulated particles ($PM_{1.4}$-TSP) along with a pre-cut inertial filter using webbed SUS fibers for the removal of fine particles ($PM_{0.5}$-$PM_{1.4}$), the present $PM_{0.1}$ inlet for the personal sampler was practical for the chemical analysis of collected particles. This sampler was proven effective even under the limitations of a small-capacity portable battery pump, which was rated at less than the minimum change for separation performance. The devised $PM_{0.1}$ personal sampler is compact and lightweight (under 1 kg including a portable battery pump), which is important for the practicality of a personal sampler. The devised $PM_{0.1}$ personal sampler has been used to evaluate the exposure to nanoparticles in various environments and results were reported in chapter 3.

Chapter 3

Exposure Assessment of Aerosol Nanoparticles and Chemical Compounds in Living and Working Environments

3.1 Introduction

In recently years, there are numerous studies showing the health risk of airborne particle exposure in regards to aerodynamic particle size, which including the respiratory and cardiovascular diseases (Bolch et al., 2001; Hussain et al., 2011; Warheit, D.B., 2004; Ward and Ayres, 2004). The relation between ambient particle concentrations and personal exposure of particles is important in order to evaluate human health effects. However, these issues have been difficult to address since personal exposure is affected by not only the ambient particle concentration but also by human activity patterns by time. It has been shown in many studies that ambient particle concentration is a poor indicator of personal exposure because concentrations in the breathing zone can be different for diverse environments (Chang et al., 1999; Johannesson et al., 2007; Lachenmyer, 2000; Oglesby et al., 2000; Wallace, 1996; Wilson and Brauer, 2006). Therefore, the most accurate way to determine personal exposure is to use personal samplers for monitoring directly pollutants in the breathing zone of the individuals.

However, several studies reported personal exposure of fine particles: $PM_{2.5}$ or PM_1 there are few studies on evaluation of personal exposure to nanoparticles, or $PM_{0.1}$. Nanoparticle exposure in living and working environment, are the great interest as the influence at sampling locations with different several activities and also surrounding environment. Epidemiology studies reported particles and chemical compositions from living and working environment, is dominant adverse health effect to workers and also resident population, such as cotton dust from a textile factory, cigarette smoke particles, vehicle road dust and pigment dusts and their chemical compounds from screen printing factory (Behera et al., 2004; Hata et al., 2013 (a); Kiurski et al., 2013; Kobayashi et al., 2004; Morawska et al., 2008; Moreland, et al., 2011; Phillips, K. and Bentley, M.C., 2001).

Carbonaceous compounds, including organic carbon (OC) and elemental carbon (EC), are major components of ambient aerosols in urban and rural atmospheres and significant important roles on radiative transfer, health effects, and atmospheric chemistry. The major sources of EC are incomplete burning of biomasses and fossil fuels while OC can be directly emitted from sources or produced from chemical reactions involving gaseous organic

precursors.

The aim of this work is to show airborne particle exposure reach to nanoparticles using devised personal samplers and chemical components; polycyclic aromatic hydrocarbons (PAHs) and carbons in living and working environment. The characteristic of nanoparticle exposure with associated carbonaceous compounds of sampling locations are summarized and discussed.

3.2 Devices for Evaluation of Personal Exposure

In this study, two main types of devised personal samplers based on the inertial filter technology, as a challenge to evaluate exposure to aerosol nanoparticles in the breathing zone, were used for the field application. The first type of devised personal sampler was referred to "Personal Nanosampler" consists of two stages of inertial filters with the best cutoff size at 140 nm. To evaluation of personal exposure reach to nanoparticles including locations of high concentration of huge particles, the second type of the personal sampler, which was referred to "$PM_{0.1}$ Personal Sampler", was developed. The $PM_{0.1}$ personal sampler consists of two stages of inertial filters with 100 nm cutoff size of a layered mesh inertial filter and two stages of pre-cut impactors. The specification of the personal sampler was shown in Table 3.1.

Table 3.1 Specification of the personal sampler

Type of Personal Sampler	Inlet Type	Cut-off Size (nm)				Flow Rate (L/min)
		The 1st Stage of Pre-cut Impactor	The 2nd Stage of Pre-cut Impactor	Pre-cut Inertial Filter	Main Inertial Filter	
$PM_{0.2}$ Personal Sampler	$PM_{0.7/0.2}$	-	-	700	200	6
$PM_{0.14}$ Personal Sampler	$PM_{0.7/0.14}$	-	-	700	140	6
$PM_{0.1}$ Personal Sampler	$PM_{4/1/0.45/0.1}$	4000	1000	450	100	5
	$PM_{5.6/1.4/0.45/0.1}$	5600	1400	450	100	5
	$PM_{10/2.5/0.45/0.1}$	10000	2500	450	100	5

3.2.1 $PM_{0.2}$ Personal Sampler

The $PM_{0.2}$ personal sampler (Furuuchi *et al*., 2010) can be used to collect particles in >700nm, 200-700 nm and <200 nm size range. Webbed stainless steel fibers (Nippon Seisen Co. Ltd., felt type, SUS-304) were packed in a circular nozzle using a polyoxymethylene (POM) for a pre-inertial filter (d_f =13.5 μm, fiber loading = 14.7-18.2 mg) and for a main inertial filter (d_f =9.8 μm, fiber loading = 3.2-3.5 mg). The 47 mm diameter quartz fiber filter

(Pallflex, 2500QAT-UP) was located downstream the main inertial filter as a backup filter. The $PM_{0.2}$ personal sampler was setup at a breathing zone of volunteers, which connected to a portable personal pump (SKC, Leland Legacy) at 6 L/min sampling flow rate with a flexible resin tube. Under allowable of pressure drop of the battery pump (5.7 kPa at 6 L/min), the $PM_{0.2}$ personal sampler can be collected sufficient particle amount for analysis of particle bound-PAHs after 6-8 hours of sampling. A schematic diagram of the $PM_{0.2}$ personal sampler is shown in Fig. 3.1 (a).

3.2.2 $PM_{0.14}$ Personal Sampler

The $PM_{0.14}$ personal sampler was developed by Furuuchi *et al*. (2010) for collect particles in >700nm, 140-700 nm and <140 nm size range. The webbed stainless steel fibers (Nippon Seisen Co. Ltd., felt type, SUS-304) (d_f =9.8 μm) were packed in a POM circular nozzle for 20.4-22.7 mg of fiber loading for a pre-inertial filter, while the 5.6 μm diameter of the SUS fiber were used for 1.6-4.2 mg for a main inertial filter. The 47 mm diameter quartz fiber filter (Pallflex, 2500QAT-UP) was used to collected particles <140 nm downstream the main inertial filter as a backup filter. The $PM_{0.14}$ personal sampler was operated at 6 L/min by a portable personal pump (SKC, Leland Legacy). A schematic diagram of the $PM_{0.14}$ personal sampler is shown in Fig. 3.1 (a).

3.2.3 $PM_{0.1}$ Personal Sampler

Fig. 3.1 (b) shows the $PM_{0.1}$ personal sampler developed by the authors (Thongyen et al., 2013, 2014) based on the inertial filter technology (Otani et al., 2007 and Eryu et al., 2009), which was used for the evaluation of exposure to $PM_{0.1}$ particles. The $PM_{0.1}$ personal sampler consists of two stage pre-cut impactors, a pre-cut inertial filter, a main inertial filter and a backup filter, could collect particles for selected different particle size range by changing a cover of the pre-cut impactors with a different inner diameter size of inlet ($PM_{4/1/0.45/0.1}$: 1000-4000 nm, 450-1000 nm, 100-450 nm and <100 nm, $PM_{5.6/1.4/0.45/0.1}$: 1400-5600 nm, 450-1400 nm, 100-450 nm and <100 nm, and $PM_{10/2.5/0.45/0.1}$: 2500-10000 nm, 450-2500 nm, 100-450 nm and <100 nm). The surface of an impaction plate of 1st stage of the pre-cut impactor was covered by silicon grease (Dow Corning, 03253589) to a uniform thickness around 0.2 mm while a 10 mm diameter of glass fiber filter (Pallflex, T60A20) was attached on an impaction plate of 2nd stage. The pre-cut inertial filter with 450 nm cutoff size, or webbed SUS fibers packed in a circular nozzle was set downstream of the pre-cut

impactors. To separate $PM_{0.1}$ particles, the main inertial filter, or layered mesh TEM grids sandwiched by spacers with circular hole in an aluminum cartridge was used to collect 100-450 nm. The $PM_{0.1}$ particles were collected on a 47 mm diameter quartz fiber filter (Pallflex, 2500QAT-UP). The outlet of the $PM_{0.1}$ personal sampler was connected to a portable battery pump (Hario Sci., HSP-5000) at 5 L/min sampling flow rate with a flexible resin tube. The $PM_{0.1}$ personal sampler, which was setup on volunteers in the breathing zone or the sampling locations, was operated at a rather small pressure drop (~7.7 kPa) and under allowable pressure drop of the portable pump (maximum at 15 kPa, 5 L/min).

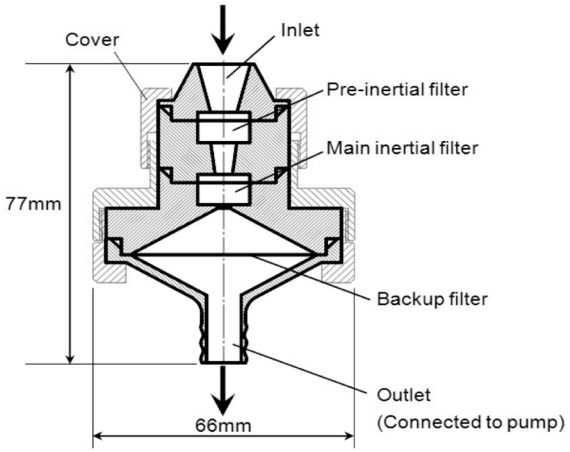

(a) $PM_{0.2}$ Personal Sampler ($PM_{0.7/0.2}$) and $PM_{0.14}$ Personal Sampler ($PM_{0.7/0.14}$)

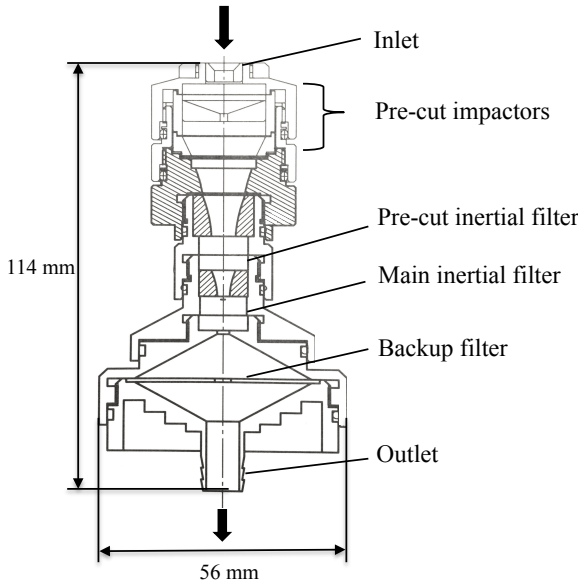

(b) $PM_{0.1}$ personal sampler ($PM_{5.6/1.4/0.45/0.1,}$ $PM_{4/1/0.45/0.1}$ and $PM_{2.5/1/0.45/0.1}$)

Fig. 3.1 Schematic diagram of personal samplers.

3.3 Environments Discussed

To discuss the personal nanoparticle exposure due to influence of different locations and surrounding activities, the samplings were conducted in Thailand, Cambodia, China and Japan using the personal sampler as a practical field application, which were classified to roadside and on road environments, smoking environments, exposure during daily activities, and working environments. The sampling information of evaluation of personal exposure was shown in Table 3.1.

3.3.1 Roadside and on Road Environments

Vehicle exhaust is the major source of ultrafine particle pollution in urban environments (Harrison et al., 1999; Shi and Harrison, 1999; Shi et al., 1999; Shi et al., 2001; Wahlin et al., 2001). Particles emitted from diesel engines are in the size range 20–130 nm (Kittelson, 1998; Ristovski et al., 2006) and from petrol engines in the range 20–60 nm (Harris and Maricq, 2001). Moreover, Morawska et al. (1998) found that a large fraction of the particle number concentration in urban air is found in the ultrafine particle size range. Therefore, the evaluation of personal exposure of drivers, pedestrians or passengers is significant important to assess to their health risk. Although previous several studies have been performed at roadsides and in road tunnels (Marr et al., 1999), the study of personal exposure to nanoparticles at roadside and on road environments was still lack.

Sidewalk along a road tunnel ($PM_{0.1}$， $PM_{0.14}$)

The sidewalk sampling was conducted in a Sakiura-Wakunami tunnel at the middle tunnel and the west-side tunnel mouth, Kanazawa, Japan, which is located on the Kanazawa outer-ring road with 667 m of total length and a 90 m2 cross-sectional area for 7 m wide of two-lane traffic, following the previous study (Hata et al., 2013). The sampling location was shown in Fig. 3.2. To comparison with a sampling site were no influencing emission sources, ambient particles at the balcony of the 6th floor of a seven-story building at Kanazawa University, 1.3 km northeast from the tunnel, was sampled. This location was no influencing emission sources around site.

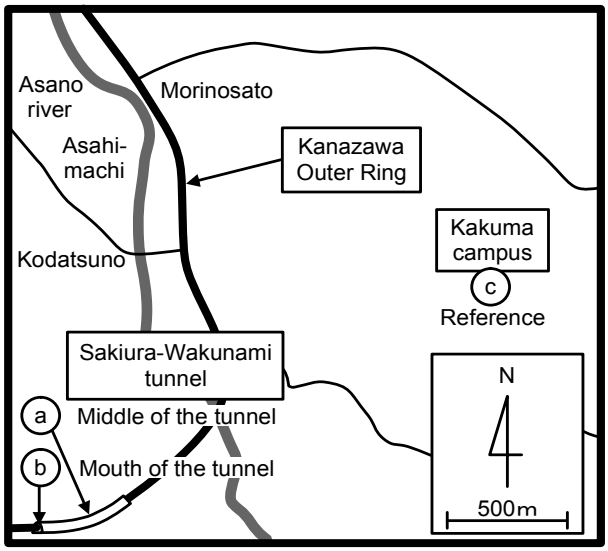

Fig. 3.2 Sampling locations for evaluation of personal exposure at sidewalk along road tunnel.

Roadside, Bus stop ($PM_{0.14}$)

The personal exposure at Musashigatsuji bus stop in downtown of Kanazawa, Japan was evaluated using the $PM_{0.14}$ personal sampler. The bus stop, where is located in front of Omicho fresh market, is always crowded in a rush hour of weekday and in a daytime of weekend. The samples were collected around 7 hours in a weekday with high density of bus and in a weekend with high density of diesel cars. Not only ultrafine particles of personal exposure from vehicle exhaust but also particle-bound PAHs were investigated to the BaP toxic equivalent concentration (BaP_{TEQ}).

Roadside, Bangkok ($PM_{0.1}$)

A roadside sampling site was set on the 3 m-wide sidewalk of five-lane traffic of a Lanluang main road, 5 m from Lanluang intersection at the central of Bangkok, Thailand, which was traffic congestion with cars, buses and motorcycles through sampling period to evaluate the influence of vehicle exhaust. During a sampling, there was raining lightly in the afternoon (~1h).

On Road, Shenyang ($PM_{0.1}$)

The on road sampling was conducted at roadside in Shenyang city, China, as a fixed site to evaluate particle concentration from vehicle exhaust. While the particle exposure in the breathing zone of a taxi driver in Shenyang was evaluated during driving, when opened-all windows to compare particle concentration with a sample at a roadside in Shenyang city.

On Road, Phnom Penh ($PM_{0.1}$)

The nanoparticle exposure of a tuk-tuk driver was sampled during the 43.1 kilometer driving in downtown of Phnom Penh pass through Institute of Technology of Cambodia (ITC) and Phnom Penh International Airport, Cambodia to evaluate the influence of vehicle exhaust directly influences the driver.

3.3.2 Smoking Environments (Passive Smoking)

Environmental tobacco smoke (ETS) or passive smoking has been reviewed about their adverse effect of exposure, such as lung cancer and heart disease. Because there are over 4000 compounds in tobacco smoke and over 60 suspected human carcinogens, such as polycyclic aromatic hydrocarbon (PAHs) (Chan-yeung and Dimich-ward, 2003; Jaakkola and Jaakkola, 1997; US.EPA, 1992). To provide the information of ETS exposure and compare with particle exposure from roadside and on road environments, the evaluation of ETS exposure in this study was conducted indoor of a public place: train cabin, a private place: in house, and also outdoor: in a campus of university.

Smoking cabin ($PM_{0.2}$)

Exposure of passengers to ultrafine particles in a cabin of a train operated by JR West Co. Ltd., where passengers were allowed to smoke, was evaluated. A volunteer sat on a seat for a round trip from Kanazawa to Osaka, Japan, carrying a personal sampler with an inlet no.1 in the breathing zone. When the volunteer left the seat, e.g., for a toilet outside the cabin, the running sampler was run left on the seat. Although the train cabin was ventilated and some fresh air could flow through doors when passengers walk through, the cabin air was always contaminated by cigarette smoke. Most of the ultrafine particles should be from cigarette smoke, probably as a function of the number of smoking passengers.

Smoker's house ($PM_{0.1}$)

Sampling was collected inside a smoker's house at Lampang province, Thailand. There was an occupant, who smoking 3 rolls of traditional cigarette of the northern Thailand: tobacco leaves in a dried banana leaf roll (Fig. 3.3), during sampling period. The $PM_{0.1}$ personal sampler was set in a living room at the second floor of the opened-window woodhouse. The occupant activities along the sampling in the house were cooking with electric stove, eating and peeling tamarind that were not significant for particle emission. There was no influence of other particle sources outside the smoker's house. The major of particle source in the house should be the smoking particles of traditional cigarette.

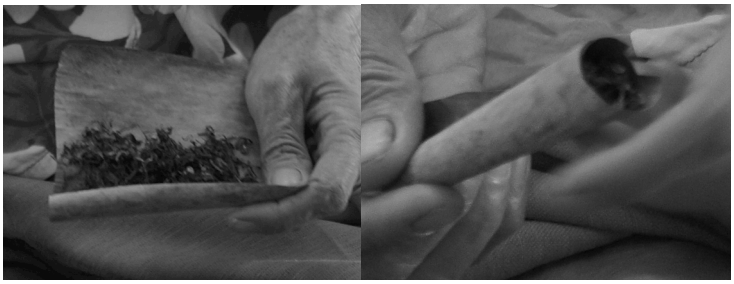

Fig. 3.3 Cigarette using dried banana leaves.

Smoker's Breathing Zone ($PM_{0.1}$)

Particle exposure in the breathing zone of a smoker, who smoking 4 rolls of cigarettes with paper rolls, was evaluated using the $PM_{0.1}$ personal sampler. The sampler was set on a volunteer during smoking at a smoking booth in a Kakuma campus, Kanazawa University, Japan. The smoking booth is located on the ground floor outdoor between two parallel 7th floor-story buildings with wind ventilation. Surroundings of the smoking booth area, there are the parking lot for ~200 cars (~100 m far from the smoking booth and behind the 7th floor-story building), lawn between the two buildings, a pathway between two buildings and to the parking lot. Therefore, the particles to nano-size range should be from cigarette smoke.

3.3.3 Exposure during Daily Activities

To discuss the influence of surrounding environment correspond with background concentration, the exposure during daily activities in Phnom Penh, Cambodia were evaluated.

Phnom Penh ($PM_{0.14}$)

Samplings were conducted to evaluate personal exposure during a daily life of a student in Phnom Penh, Cambodia in a weekday and a holiday. The weekday sampling was operated during a student as a volunteer went to outside, drove a motorcycle between a volunteer's house, Newton Thilay school (NTS), and Institute of Technology of Cambodia (ITC). While the holiday sampling was collected during a volunteer stayed at a volunteer's house, drove a motorcycle to downtown of Phnom, and walked around Phnom Penh downtown area.

Kanazawa ($PM_{0.14}$)

Particle exposure of student was evaluated during a daily life in Kanazawa, Japan. The sampling was operated during a student as a volunteer went to outside from an apartment, drove a car between a student's apartment to Kanazawa University.

Hat Yai ($PM_{0.14}$)

Samplings were conducted to evaluate personal exposure during a daily life of a student in Hat Yai, Songkhla provience, Thailand in a weekday and a weekend.

3.3.4 Working Environments

Rubber sheet smoking factory ($PM_{0.14}$)

The Saikao Cooperative, an RSS factory located in the Muang district of Songkhla province, Thailand, was selected for investigation of exposure of workers to smoke particles and particle-bound PAHs. Five from six workers employed in this RSS factory voluntarily participated as volunteers. Ultrafine particles and PAHs should be from biomass fuel burning, which was a part of a process of rubber smoke sheet production using rubber woods as a typical working environment polluted by smoke particles.

Textile factory ($PM_{0.1}$)

Environment of textile factory inside spinning process room, where spinning machines were operated, was investigated. The $PM_{0.1}$ personal sampler was used to evaluate personal exposure of a worker, who working for moving up yarn tanks from a storage to the spinning machines, connecting yarn of the spinning machines and cleaning the working area floor. Most of the ultrafine particles should be from process of spinning machines.

Print screen factory ($PM_{0.1}$)

Print screen factory, which is located in Bangkok, the central region of Thailand, was sampled to compare the influence of different types of factories. Personal nanoparticle exposure was evaluated at a breathing zone of a worker, who worked at a screen printer during a print screen process of plastic shower caps on the third floor with opened-all windows of a four-story building. The particles from outside the factory and carbon compounds from liquid color in the print screen process were ventilated by wind dilution through opened windows.

TiO_2 nano-powder factory ($PM_{0.1}$)

Worker, who filled TiO_2 particles into a bag, was evaluated to the exposure of nanoparticle. During working, the worker sat on a seat at a packing area. Above the seat of the worker, there was a hood that operated for sucking a surrounding air to reduce their dispersion of particles.

Paint factory ($PM_{0.1}$)

Sampling was conducted to evaluate personal exposure in the breathing zone of a worker of a paint factory, who poured color powder from a plastic bag into a mixing tank that located in the central of a paint mixing process room. There was not a hood or a particle control system to reduce particle dispersion and particle emission source near the color mixing tank or the central of factory. The major particle source to exposure of a worker came from the color powder.

3.4 Procedure

3.4.1 Filter Preparation

Filters of the personal sampler consists of a pre-inertial filter, a main-inertial filter and a backup filter, and filters of the $PM_{0.1}$ personal sampler consists of a filter for an impaction plate of pre-cut separators, a pre-cut inertial filter, a main inertial filter and a backup filter were prepared. All filters were conditioned in a chamber at temperature ~20 ^{o}C and a relative humidity ~50% for at least 48 hours before being weighed to obtain weights and then used for the sampling. All filters for carbon analysis were heated in an oven at 900 ^{o}C for 24 hours before conditioned in a chamber at the same condition before weighting and using for the sampling. After the sampling, filters were weighed after 48 hours of the same conditioning procedure.

3.4.2 Analysis of Chemical Components

Carbons

The $PM_{0.1}$ particles, which were collected on 47 mm diameter quartz fiber filters (the backup filters of the $PM_{0.1}$ personal sampler), were analyzed for carbon components using a proven thermal-optical method of OC-EC aerosol analyzer (Sunset Laboratory Inc., USA) with 25 minutes of resolution. The OC-EC aerosol analyzer was operated following the IMPROVE_TOR method (Interagency Monitoring of Protected Visual Environments_Thermal/Optical Reflectance Method). The collected sample was punched for 1 cm^2, and then placed onto the sample load position of the analyzer. Inside of the analyzer during the analysis, the sample was heated to produce four OC fractions (OC1, OC2, OC3, and OC4) in a non-oxidizing helium atmosphere, as well as three EC fractions (EC1, E2, and E3), in an oxidizing atmosphere of 2%O_2/98% He. The EC fraction was divided into char-EC

and soot-EC. Char-EC is defined as EC1 minus a pyrolyzed carbon fraction, and the soot-EC is defined as the sum of EC2 and EC3.

Polycyclic aromatic hydrocarbons (PAHs)

Fifteen different PAH compounds–Naphthalene (Nap), Acenaphthene (Ace), Phenanthrene (Phe), Anthracene (Ant), Fluorene (Fle), Fluoranthene (Flu), Pyrene (Pyr), Benzo[a]anthracene (BaA), Chrysene (Chr), Benzo[a]pyrene (BaP), Benzo[b]fluoranthene (BbF), Benzo[k]fluoranthene (BkF), Dibenz[a,h]anthracene (DbA), Indeno[1,2,3-cd]pyrene (IDP), and Benzo[ghi]perylene (BghiPe) were analyzed by HPLC (HITACHI/L-2130/2200/2300/2485) with a fluorescence detector and an Inertsil ODS-P column (5 μm, 3.0 mm diameter, 250 mm length) + acetonitrile/ultra-pure water mobile phase after ultrasonically dissolving the samples on the filter in an ethanol/benzene (1:3) solution, followed by evaporation on a rotary vacuum evaporator (Toriba et al., 2003). The average recovery efficiency for 15 components was confirmed to be 0.82 ± 0.12 (n = 3) by adding a standard reagent [Accustandard 0.2 mg/mL in CH_2Cl_2: MeOH (1:1)] to the samples (Tang et al., 2005). The values of PAHs from 3 travel blank filters were subtracted from the values determined by analysis: 8.5 ± 5 pg/cm^2 for 2–3 ring PAHs and 5.5 ± 5 pg/cm^2 for 4–6 ring PAHs (Choosong, T., 2009 and Choosong et al., 2010). These blank values were significantly less than the concentrations of each compound in all samples used.

Table 3.1: Sampling information of evaluation of personal exposure

Location	Type of Sampler	Components	Sampling Period
Roadside and on Road Environments			
(A) Sidewalk along a road tunnel			
• Middle of tunnel-1	$PM_{0.7/0.14}$	PAHs	June 3, 2009 (15h)
• Middle of tunnel-2	$PM_{5.6/1.4/0.45/0.1}$	-	July 8-9, 2013 (10.5h)
• Mouth of tunnel	$PM_{5.6/1.4/0.45/0.1}$	-	July 8-9, 2013 (24h)
• Background	$PM_{5.6/1.4/0.45/0.1}$	-	April 23-24, 2013 (24h)
(B) Roadside, Bus stop			
• Weekday	$PM_{0.7/0.14}$	PAHs	October 1, 2009 (12h)
• Weekend	$PM_{0.7/0.14}$	PAHs	October 4, 2009 (12h)
(C) Roadside, Bangkok	$PM_{5.6/1.4/0.45/0.1}$	Carbons	March 3, 2013 (4h)
(D) On road, Shenyang			
• Roadside	$PM_{10/2.5/0.45/0.1}$	-	August 24, 2013 (7.5h)
• Taxi driver	$PM_{10/2.5/0.45/0.1}$	-	August 24, 2013 (2.5h)
(E) On road, Phnom Penh	$PM_{0.7/0.14}$	-	October 5, 2011 (6h)
Smoking Environments (Passive Smoking)			
(F) Smoking cabin	$PM_{0.7/0.2}$	PAHs	January 10, 2009 (5.5h)
(G) Smoker's house	$PM_{5.6/1.4/0.45/0.1}$	Carbons	March 9, 2013 (5h)
(H) Smoker	$PM_{5.6/1.4/0.45/0.1}$	Carbons	January 16, 2013 (3h)
Exposure during Daily Activities			
(I) Phnom Penh			
• Weekday	$PM_{0.7/0.14}$	-	November 1-4, 2011 (3h)
• Weekend	$PM_{0.7/0.14}$	-	October 29-30, 2011 (24h)
(J) Kanazawa	$PM_{0.7/0.14}$	-	(39.5h)
(K) Hat Yai			
• Weekday	$PM_{0.7/0.14}$	-	(2.5h)
• Weekend	$PM_{0.7/0.14}$	-	(13h)
Working Environments			
(L) Rubber sheet smoking (RSS) factory			
• RSS factory-1	$PM_{0.7/0.2}$	PAHs	September 2008 (7 samples)
• RSS factory-2	$PM_{0.7/0.2}$	PAHs	January 2009 (4 samples)
• RSS factory-3	$PM_{0.7/0.14}$	PAHs	January 2009 (3 samples)
• RSS factory-4	$PM_{0.7/0.14}$	PAHs	February 2009 (2 samples)
(M) Textile factory	$PM_{5.6/1.4/0.45/0.1}$	Carbons	March 4, 2013 (6h)
(N) Print screen factory	$PM_{5.6/1.4/0.45/0.1}$	Carbons	March 5, 2013 (2.5h)
(O) TiO_2 nano-powder factory	$PM_{5.6/1.4/0.45/0.1}$	-	January 10, 2013 (2.5h)
(P) Paint factory	$PM_{0.45/0.1}$	-	November 16, 2012

3.5 Results and Discussion

3.5.1 Particles

Roadside and on Road Environments

The concentrations of particles fractioned by the personal sampler were shown in Fig.3.4, 3.5 and 3.6. The several studies reported that particle concentration on roadside and road environment is a function of road conditions, driving speed, vehicle types and wind speed (Sehmel et al., 1980, Nicholson et al., 1993, Goosens et al., 2009). In this study, the total particle concentration at the mouth of the tunnel was lower than the middle of the tunnel due to wind dilution. The roadside sampling point at Bangkok ~5m far from the intersection caused high concentration from traffic jam. The fraction of fine particles (140-700nm and >700nm) related to the number of heavy vehicles (643 buses in a weekday and 500 buses in a weekend during sampling period) that corresponded to the previous report (Hata et al, 2013). The personal exposure of a taxi driver was quite high by particles outside the taxi flowing through opened-windows. The tendency is clear that high fraction of large particles from road dust. This is significant to realize the health of drivers, especially where background concentration was the high level. Moreover, the results showed that the evaluation of personal exposure at the breathing zone is important from the point view of health risk.

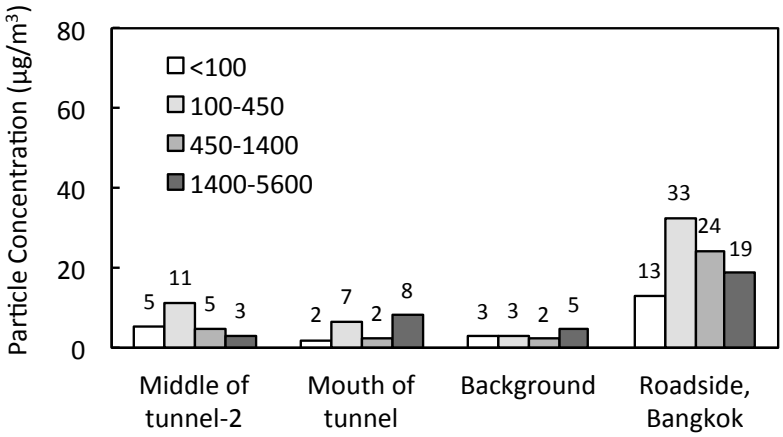

Fig. 3.4 Particle mass concentrations of collected particles at middle and mouth of tunnel, background at Kanazawa and roadside at Bangkok.

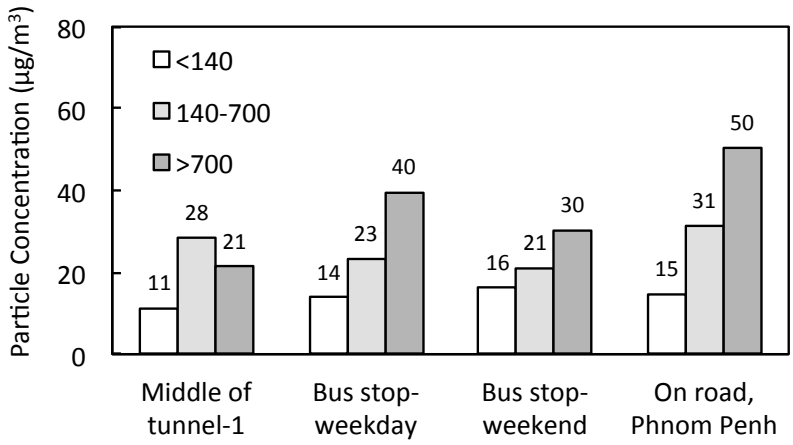

Fig. 3.5 Particle mass concentrations of collected particles at middle of tunnel, bus stop in a weekday and a weekend at Kanazawa and on road at Phnom Penh.

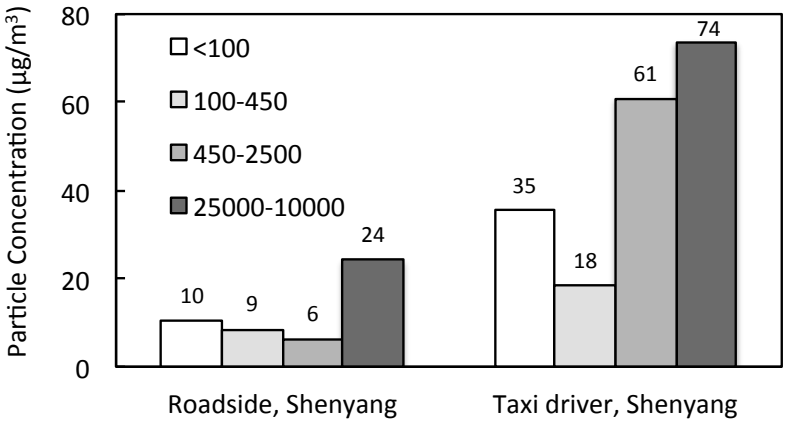

Fig. 3.6 Particle mass concentrations of collected particles at roadside and the breathing zone of taxi driver at Shenyang.

Smoking Environments

The train cabin contaminated by cigarette smoke particles was evaluated the personal exposure of a passenger. Fig. 3.7 shows the maximum concentration was in the middle range (200-700nm) and ~50% of mass ratio in the ultrafine particles (<200nm). This trend of smoke particles was not the case in a smoker's house and the breathing zone of a smoker as shown in Fig. 3.8, which particles was maximum concentration in the coarse range (1.4-5.6μm). However, the mass ratio of $PM_{0.1}$ particles at a smoker's house and the breathing zone of a smoker were still high (~30%). Total particles in a train cabin was found around 2 times of total particles at a smoker's house with opened windows and a breathing zone of smoker who

smoking outside. According to the results, the ventilation of air is an important point to decrease the personal exposure of particles.

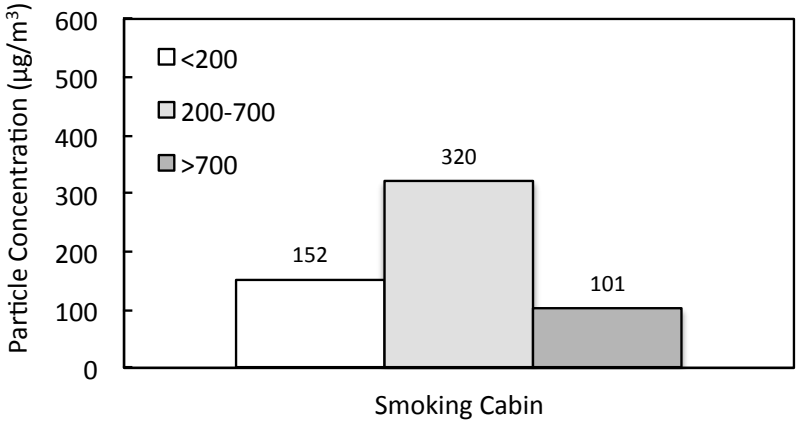

Fig. 3.7 Particle mass concentrations of collected particles at the breathing zone of train passenger in a smoking cabin.

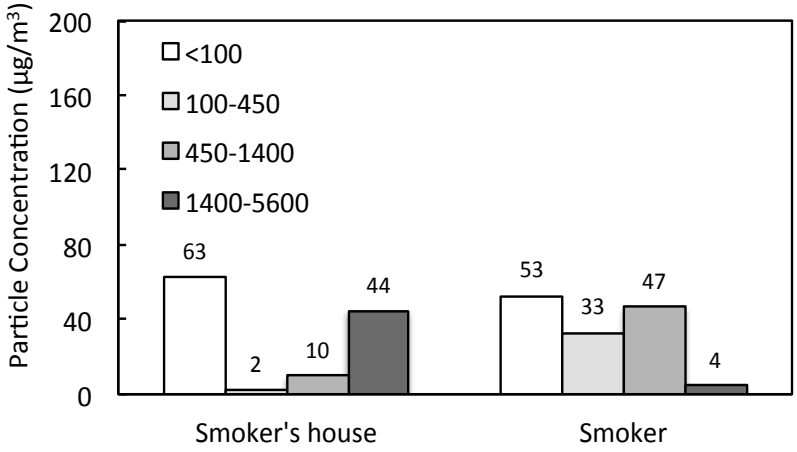

Fig. 3.8 Particle mass concentrations of collected particles at a smoker house and the breathing zone of smoker.

Exposure during Daily Activities

The personal exposure of particles during daily activities at Phnom Penh, Hat Yai and Kanazawa were shown in Fig. 3.9. Sampling in a weekday during riding a motorcycle between a volunteer's house, Newton Thilay school (NTS), and Institute of Technology of Cambodia (ITC), and staying at ITC. The sampler was turned off during a class. The exposure found the peak at middle size (140-700nm). While the exposure in a weekend with ~3h for travel by motorcycle, ~18h for staying at a home near roadside where was not air conditioner in a house, and ~3h for walking riverside in a city area, the maximum fraction of

particles was in a coarse size (>700nm). The behaviour of particle exposure in a weekend, which was high fraction of coarse particles, corresponded with the results was collected at the breathing of a Tuktuk driver in Phnom Pehn. Therefore, vehicle exhaust may a major particle source of particle exposure in a weekend. The personal exposure of students at Kanazawa and Hat Yai were reported as same as the personal exposure at Phnom Pehn, were high mass fraction of coarse particles because of influence of road dust and vehicle exhaust .

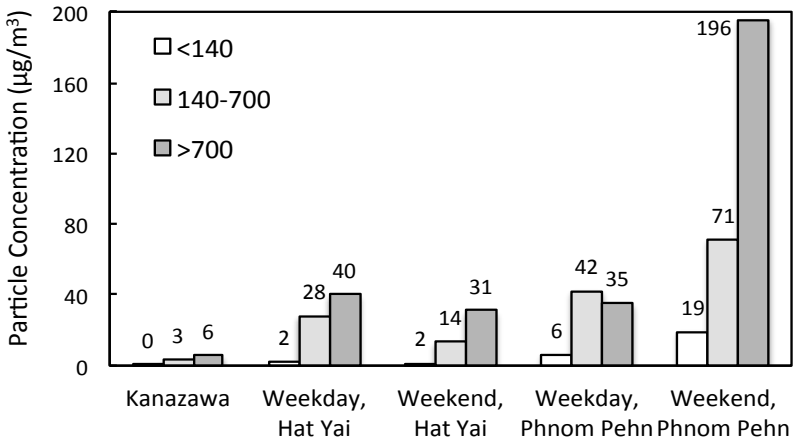

Fig. 3.9 Particle mass concentrations of collected particles of a daily life in a weekday and a weekend at Phnom Penh.

Working Environments

Fig. 3.10 shows particle exposure of workers of Rubber sheet smoking (RSS) in September 2008 (RSS factory-1) and January 2009 (RSS factory-2), measuring by the $PM_{0.2}$ personal sampler. The exposure of particles by fractionated size was unclear when the coarse particles (>700nm) were the large fraction of September sampling but they was the small fraction of January sampling. The reasons of this behavior of exposure was not the characteristic of RSS process such as production quantity of RSS, the whether condition at RSS factory was the factor of particle exposure (Choosong et al., 2010). The exposure of January and February as shown in Fig.3.11 was evaluated in same season, showed similar trend of particle concentration by size. The results in this study also corresponded with the previous report. Fig. 3.12 shows the particle concentrations was found to be significant at a textile factory, especially coarse particles (450-1400 nm), which found 50% mass fraction because of residue yarn from the operating spinning machines. The exposure of workers of a TiO_2 nano-powder factory was found to be important in coarse particles (Fig. 3.12) because the nanoparticles were high density in the air, became the coarse particles. Fig. 3.13 shows

the particle exposure in the case of a worker of a paint factory using $PM_{0.1}$ personal sampler without two stages of pre-cut impactors. More than 50% of particles was in >450 nm size range. Because of the high concentration of huge particles, it was a cause of coagulation problem of the sampler. Therefore, the $PM_{0.1}$ personal sampler with two stages of pre-cut impactors was recommended to use in a case of high concentration of huge particles.

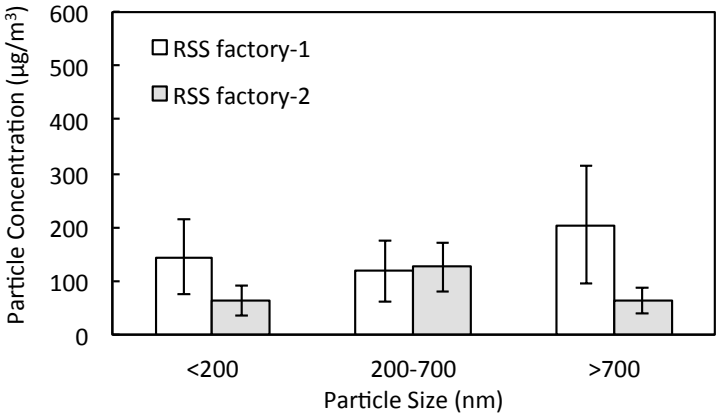

Fig. 3.10 Particle mass concentrations of collected particles at the breathing zone of workers of Rubber sheet smoking (RSS): factory RSS factory-1 (September 2008) and RSS factory-2 (January 2009).

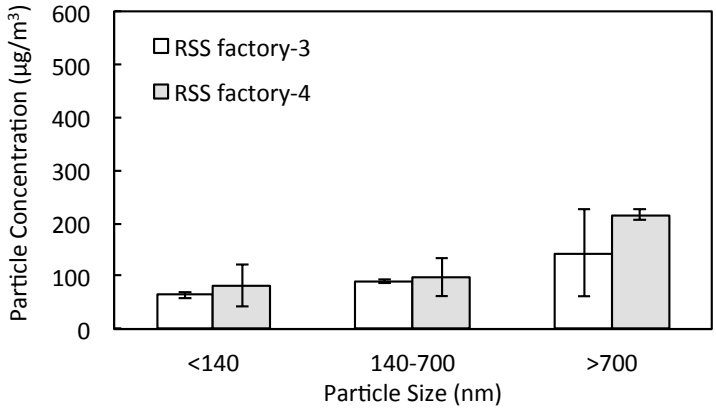

Fig. 3.11 Particle mass concentrations of collected particles at the breathing zone of workers of Rubber sheet smoking (RSS): RSS factory-3 (January2009) and RSS factory-4 (February 2009).

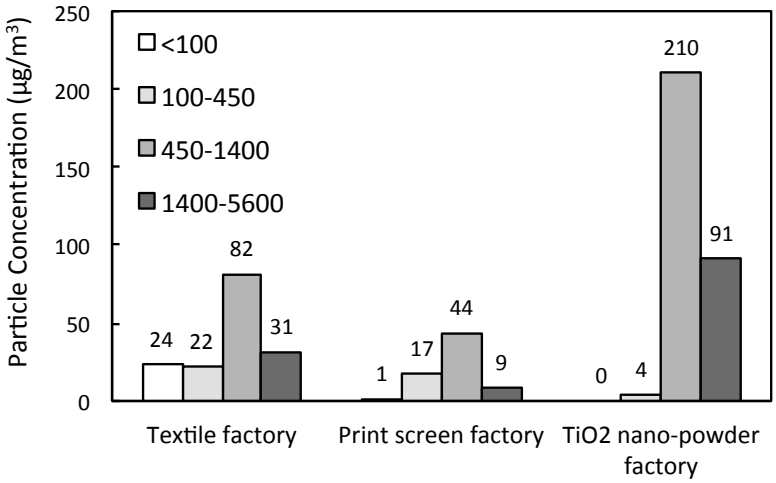

Fig. 3.12 Particle mass concentrations of collected particles at the breathing zone of workers of a textile factory, a print screen factory, and a TiO_2 nano-powder factory.

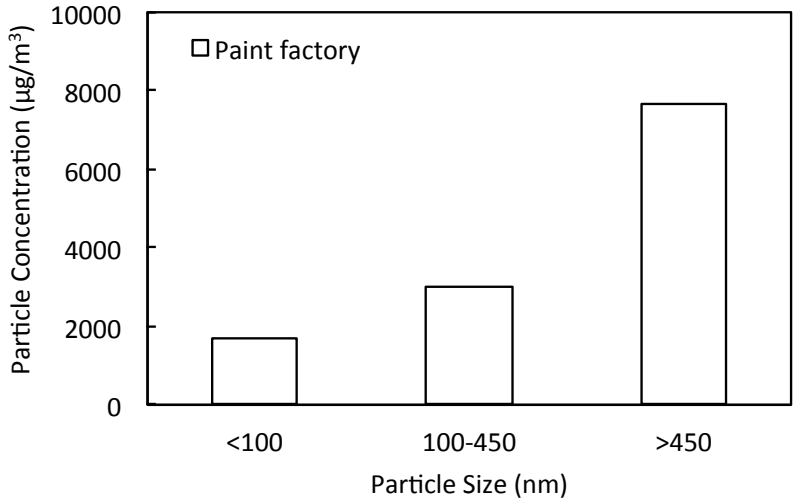

Fig. 3.13 Particle mass concentrations of collected particles at the breathing zone of worker of a paint factory.

3.5.2 Carbon Components

Fig. 3.14 (a) shows the highest OC concentration in print screen factory because the colour in the process of production consists of oganic compounds in the colour using components. Fig. 3.14 (c) shows the ratio of the OC/EC in nanoparticles at roadside, Bangkok was 28.4. While the previous studies reported that the OC/EC ratios of fine particles in the tunnel sampling and diesel vehicles were 0.56 and 0.28-0.92, respectively (Huang et al., 2006; Allen et al, 2001). Schauer et al. (1999, 2002) found the OC/EC in $PM_{1.8}$ for diesel and gasoline vehicles was about 0.6 and 4.3, respectively. In this study, source of roadside

sampling in this study was vehicle exhaust. However, the OC/EC ratio was higher than the report of the previous studies. For smoking environments, the OC/EC ratio shows 5.5 and 16.3 at the smoker's breathing zone and smoker's house. Because of different type of cigarette, the ratio of OC/EC in smoker's house, where a volunteer was smoking tobacco using dried banana leaves, was higher. Because the kind of smoking using dried banana leaves resembled with biomass burning, the OC/EC in this study corresponded with the previous report that showed the OC/EC ratio from biomass burning was higher than 8.

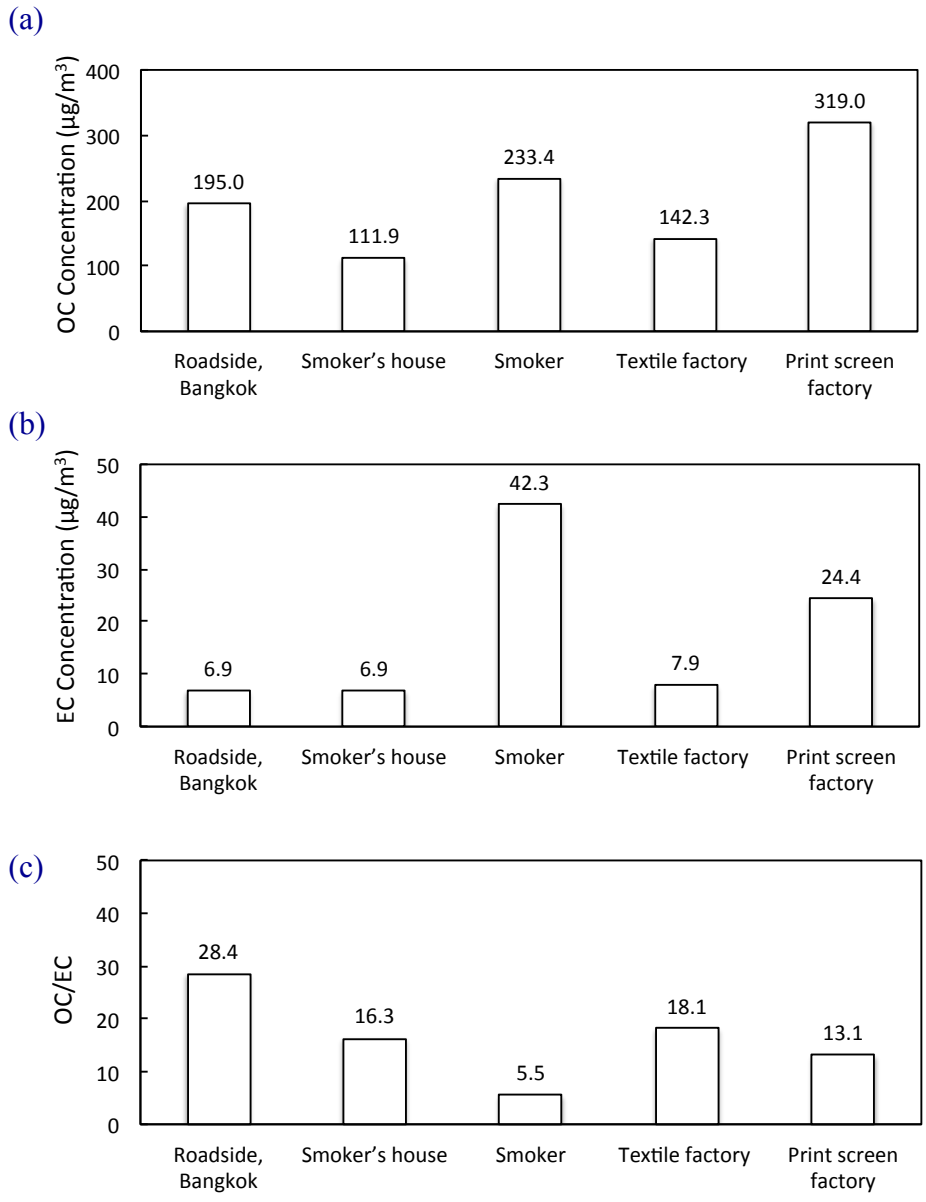

Fig. 3.14 Carbon components of collected $PM_{0.1}$ particles (a) OC (b) EC and (c) OC/EC.

3.5.3 PAHs

Fig. 3.15 shows particle-bound 4-6 rings PAHs concentration at roadside environments, which found similar trend of high fraction in 140-700 nm particles of all sampling locations. For working environments in the RSS factory both of particles collected using the $PM_{0.2}$ personal sampler (Fig. 3.15) and the $PM_{0.14}$ personal sampler (Fig. 15), the maximum fraction of particle-bound 4-6 rings PAHs was in the middle size range (140-700 nm and 200-700 nm). To compare with smoking environments, the particle-bound 4-6 rings PAHs in the RSS factory was very high concentration, around 2-4 times of particle-bound 4-6 rings PAHs in a smoke cabin.

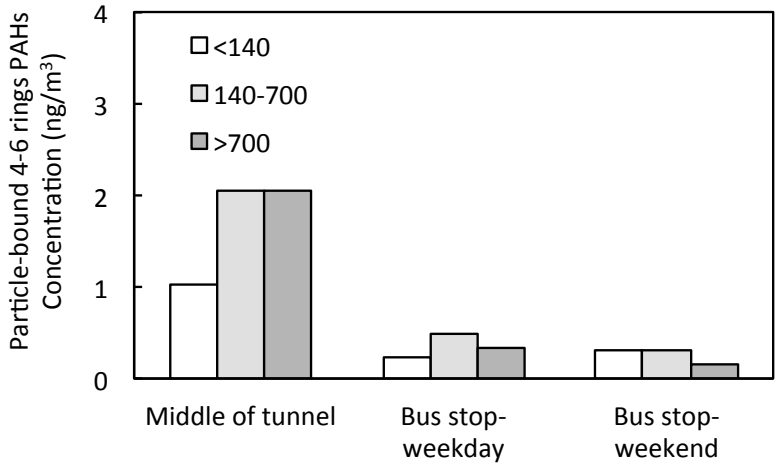

Fig. 3.15 Particle-bound 4-6 rings PAHs concentration at middle of tunnel and bus stop in a weekday and a weekend at Kanazawa.

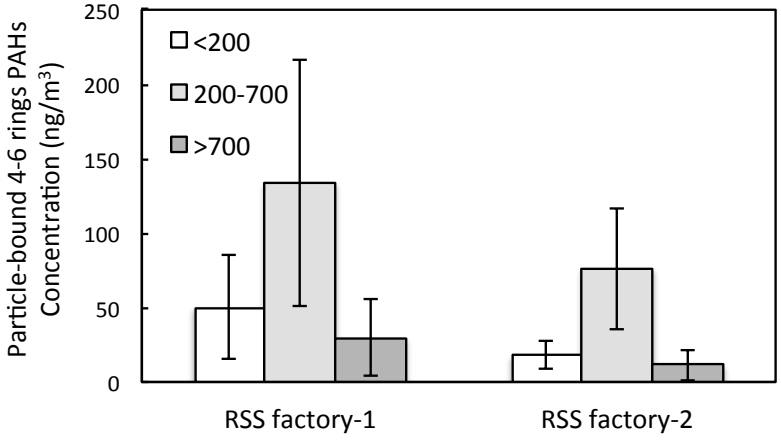

Fig. 3.16 Particle-bound 4-6 rings PAHs concentration at the breathing zone of workers of Rubber sheet smoking (RSS): RSS factory-3 (January2009) and RSS factory-4 (February 2009).

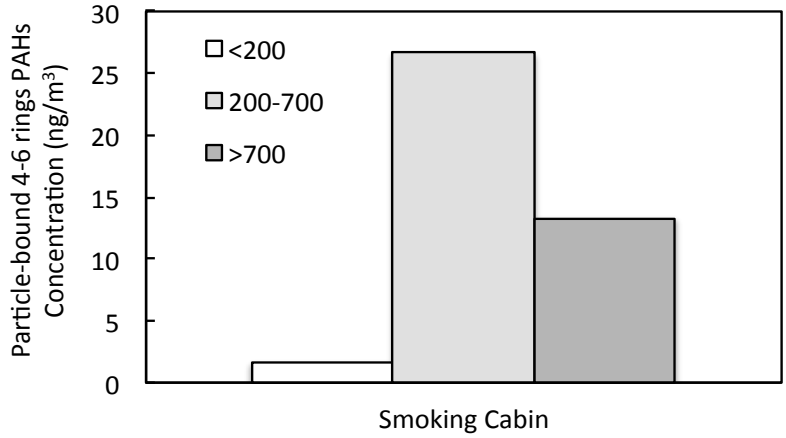

Fig. 3.17 Particle-bound 4-6 rings PAHs concentration at the breathing zone of train passenger in a smoking cabin.

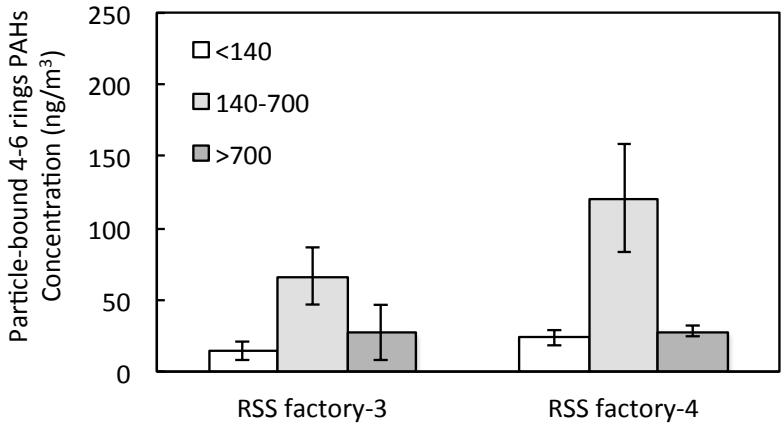

Fig. 3.18 Particle-bound 4-6 rings PAHs concentration at the breathing zone of the breathing zone of workers of rubber sheet smoking (RSS): factory RSS factory-1 (September 2008) and RSS factory-2 (January 2009).

In order to evaluate risk of particles, the toxic factor BaP_{TEQ}, the PAHs concentration normalized to the cancer potency equivalent factor of Benzo[a]pyrene or the BaP Toxic Equivalence. On roadside environments, BaP_{TEQ} mass fraction of collected particles at the middle of the tunnel was the highest in particles <140nm and 2-4 times of BaP_{TEQ} mass fraction at the bus stop (Fig. 3.19). It is different with the RSS factory, which clearly shows the high fraction of BaP_{TEQ} mass fraction in 140-700 nm and 200-700 nm as shown in Fig. 3.21 and 3.22.

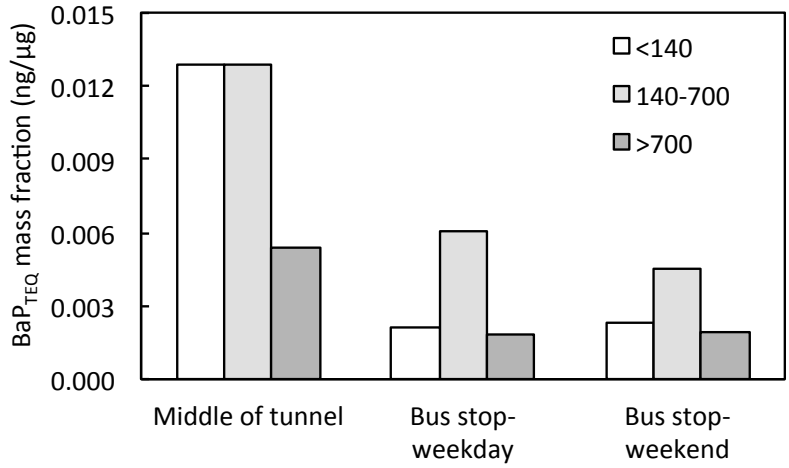

Fig. 3.19 BaP$_{TEQ}$ mass fraction at middle of tunnel and bus stop in a weekday and a weekend at Kanazawa.

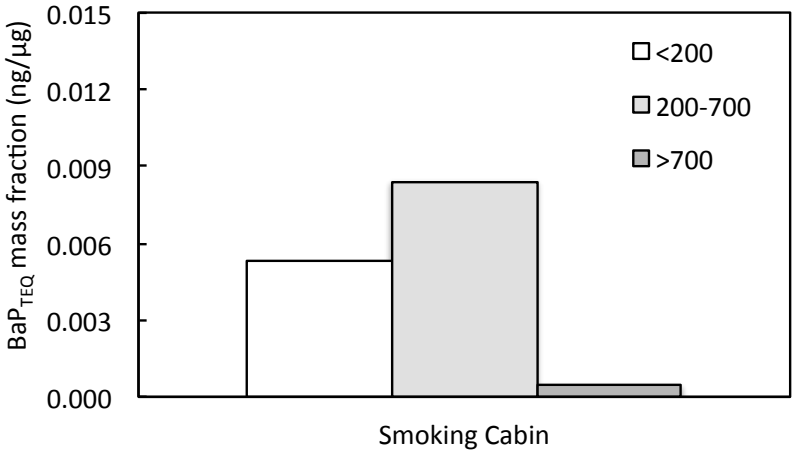

Fig. 3.20 BaP$_{TEQ}$ mass fraction at the breathing zone of train passenger in a smoking cabin.

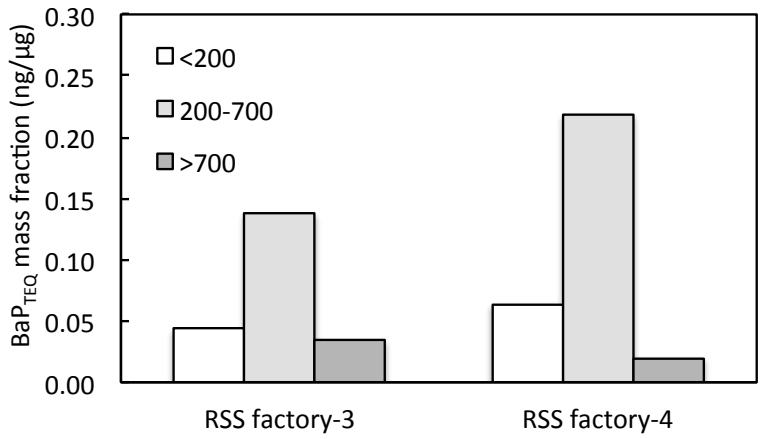

Fig.3.21 BaP$_{TEQ}$ mass fraction at the breathing zone of workers of rubber sheet smoking (RSS): RSS factory-3 (January2009) and RSS factory-4 (February 2009).

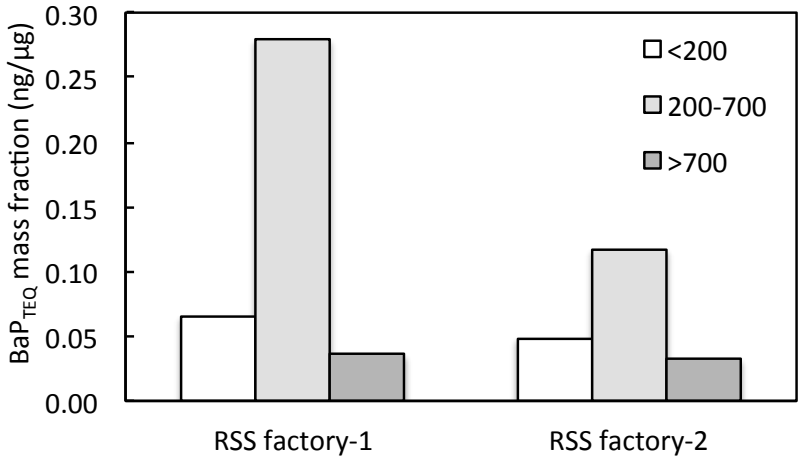

Fig. 3.22 BaP$_{TEQ}$ mass fraction at the breathing zone of train passenger.

3.6 Conclusion

The exposure to nanoparticles in living and working environments was successfully evaluated using the developed personal sampler. The assessment of personal exposure to nanoparticles and their chemical compounds were found to be important in the breathing zone of taxi drivers in Shenyang, China, a train passenger in a smoking cabin, smokers, workers of rubber sheet smoking factory and textile factory. The fraction of fine particles at a bus stop related to the number of heavy vehicles. The exposure of a taxi driver confirmed that the evaluation of personal exposure at the breathing zone is important from the point view of health risk during activities because particle exposure at the breathing zone was higher than particle concentration in the surrounding environment. The chemical compounds of particles

showed the high health risk due to rather high average of particle-bound 4-6 rings PAHs concentration at rubber sheet smoking factory. Moreover, the exposure at middle of tunnel was lower particles concentration than the exposure at a bus stop, but it found the higher health risk as BaP_{TEQ} mass fraction.

Chapter 4

Online Monitoring of $PM_{0.1}$ Number Concentration and Particle-bound Black Carbon Using $PM_{0.1}$ Inertial Filter

4.1 Introduction

The online monitoring of aerosol particles is an important aspect of the evaluation of human health and environmental effects due to varying particle concentration and their chemical compositions by time change along with different surrounding activities. There are several commercial instruments to online monitor a variation of nanoparticle number concentration by selecting particle size e.g., laser aerosol spectrometer (LAS), scanning mobility particle sizer (SMPS) and nanoscan SMPS. However, these instruments are high price cost. While the medium cost instruments such as condensation particle counter (CPC), are available on the market. The CPC can be used to online monitor the particle number concentration in a total of micro- and nano-size particles, but it is not able to select size of particles. Therefore, using a simple tool to combining with CPC to be able to monitor $PM_{0.1}$ is an approach of this study. Particle-bound black carbon (BC) has been recognized to be one of the main responsible of global warming due to light absorption (IPCC, 2007) and also harming to human health (Jansen et al., 2012). In case of online monitoring of black carbon concentration, commercial black carbon monitors are available to measure black carbon in total suspended particles (TSP) or in $PM_{2.5}$ particles such as a multi angle absorption photometer (MAAP) (Thermoscience, Model 5012). However, the black carbon monitor for measurement of BC in nanoparticles is not available and knowledge of BC in the atmosphere is still seriously lacking, especially BC in nanoparticles.

A $PM_{0.1}$ separation unit based on the inertial filter technology was designed so as to provide 100 nm of cut-off size and a dust loading capacity enough to be applied for the $PM_{0.1}$ separation in various environments including workplace and living environments. Using the devised $PM_{0.1}$ separation unit as a separator at the inlet of a condensation particle counter (CPC), a system for the online monitoring of $PM_{0.1}$ was proposed as a simple tool for nanoparticle monitoring and was applied for the ambient $PM_{0.1}$ monitoring. In addition, as an example of the online monitoring of chemical components in environmental nanoparticles, a black carbon monitor was combined with the above system and applied to the ambient $PM_{0.1}$ particles. Behavior and characteristics of ambient $PM_{0.1}$ were also discussed.

4.2 $PM_{0.1}$ Separation Unit

Fig. 4.1 shows structure of a $PM_{0.1}$ separation unit, which is a part of $PM_{0.1}$ perosnal sampler as shown the detail information in the chapter 2, which consists of the pre-cut and the layered mesh inertial filters located downstream the two stage pre-cut impactors. The $PM_{0.1}$ unit was designed as being applicable both to the online monitoring of number concentration of $PM_{0.1}$ particles and the evaluation of mass concentration of $PM_{0.1}$ so that a filter holder for a backup filter to collect $PM_{0.1}$ particles is located downstream the layered mesh inertial filter. For the monitoring application purpose, the filter holder is removed. Weight of the $PM_{0.1}$ unit is 112 g and dimensions are 6.5 cm maximum width and 11.4 cm height. These are reasonably wright and compact to be used with other instruments as CPC and etc.

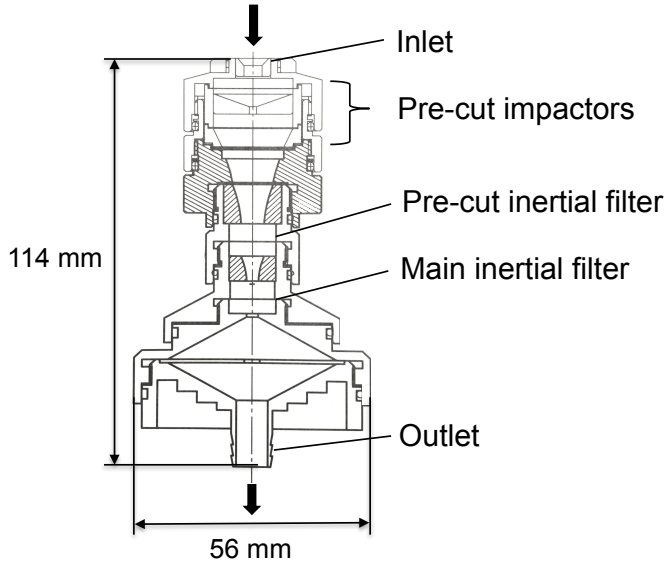

Fig. 4.1 Structure of $PM_{0.1}$ separation unit.

4.3 Proposed Monitoring System

Fig. 4.2 shows an example of a $PM_{0.1}$ online monitoring system proposed in the present study, which is the portable setup, consists of a portable CPC combined with the $PM_{0.1}$ separation unit. The air flow of 5 L/min from the $PM_{0.1}$ separation unit is sampled by a portable CPC (TSI, Model 3007) with 0.7 L/min of sampling flow rate, where $PM_{0.1}$ particles are collected on 47 mm diameter of a fibrous filter by a portable pump (HARIO, HSP-5000) with 4.3 L/min of sampling flow rate. Since the total flow rate is still enough to be used for other instruments, a scanning mobility particle sizer (SMPS), e.g., can be connected to check the separation performance of the $PM_{0.1}$ separation unit as described in the followings. Such

system can be operated because of a small pressure drop through the $PM_{0.1}$ separation unit (~ 7 kPa) and cannot be done by conventional instruments for the separation ultra-fine nanoparticle such as the low pressure impactor (LPI) operated under 60-80kPa of pressure drop.

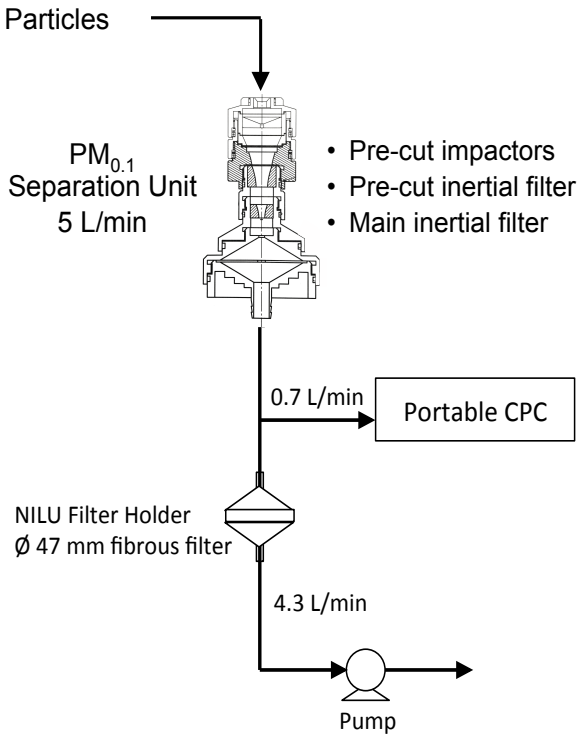

Fig. 4.2 $PM_{0.1}$ online monitoring system proposed in the present study.

Fig. 4.3 shows an example of a $PM_{0.1}$ and associated BC online monitoring system proposed in the present study, which is the stationary setup. MAAP was combined with the online monitoring system of the portable setup to determine behavior of BC in $PM_{0.1}$. The $PM_{0.1}$ particles, which were classified by the $PM_{0.1}$ separation unit with the airflow of 5 L/min, were sampled by a portable CPC (TSI, Model 3785) with 1.0 L/min of sampling flow rate. The remaining airflow (4 L/min) was added 12.7 L/min of clean air through a HEPA filter. The BC in $PM_{0.1}$ particles was measured by MAAP with 16.7 L/min of sampling flow rate. Using this system as Fig.4.2 and Fig. 4.3, chemical component of particles collected on the filter can be analyzed to discuss detailed characteristics of environmental aerosol nanoparticles.

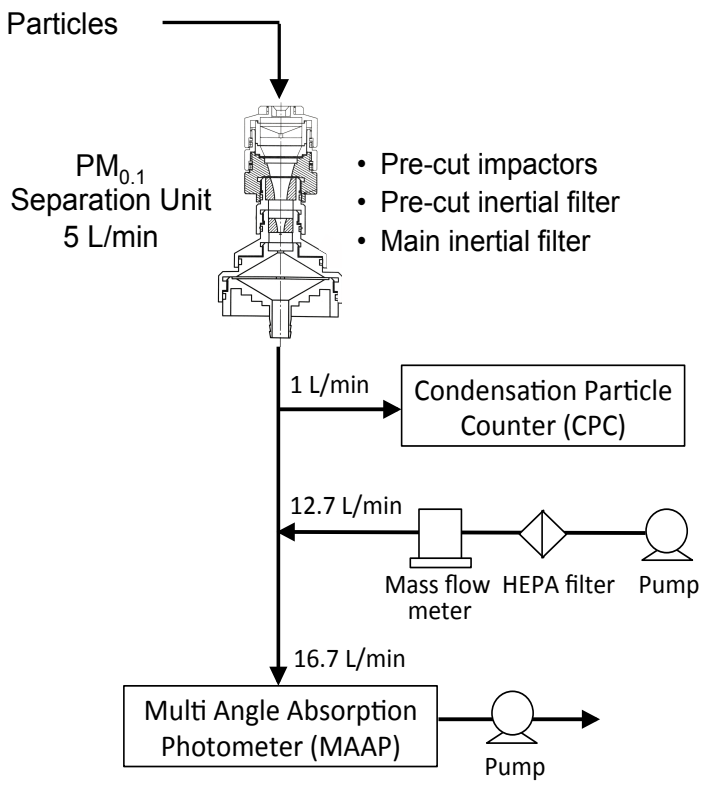

Fig. 4.3 $PM_{0.1}$ and associated BC online monitoring system proposed in the present study.

4.4 Experiments

4.4.1 Setup and Validation of $PM_{0.1}$ Online Monitoring System

Based on the idea shown in Fig. 4.2 and Fig. 4.3, the $PM_{0.1}$ online monitoring system was setup and the validation test of the system was conducted in a laboratory. Fig.4.4 shows a monitoring system consisting of the $PM_{0.1}$ unit without a filter holder and CPC (TSI, Model 3785) for the number concentration of $PM_{0.1}$ particles (1 L/min of sampling flow rate). This system is the simplest configuration for the validation. Hence, two set of SMPS (TSI, Nanoscan 3910 and TSI, SMPS 3034) were installed to measure both concentration of particles before and after the $PM_{0.1}$ unit to confirm the separation performance of the unit during the monitoring duration.

The poly-dispersed $ZnCl_2$ particles were generated following a reported procedure (Furuuchi, M et al., 2010). After classifying generated $ZnCl_2$ particles by a differential mobility analyzer (DMA), mono-dispersed $ZnCl_2$ particles were used as the test particles. Then, the $ZnCl_2$ particles were diluted by air through a HEPA filter and supplied to the $PM_{0.1}$

separation unit. The particle size distribution of upstream and downstream of the $PM_{0.1}$ separation unit was measured using SMPS to confirm the separation performance.

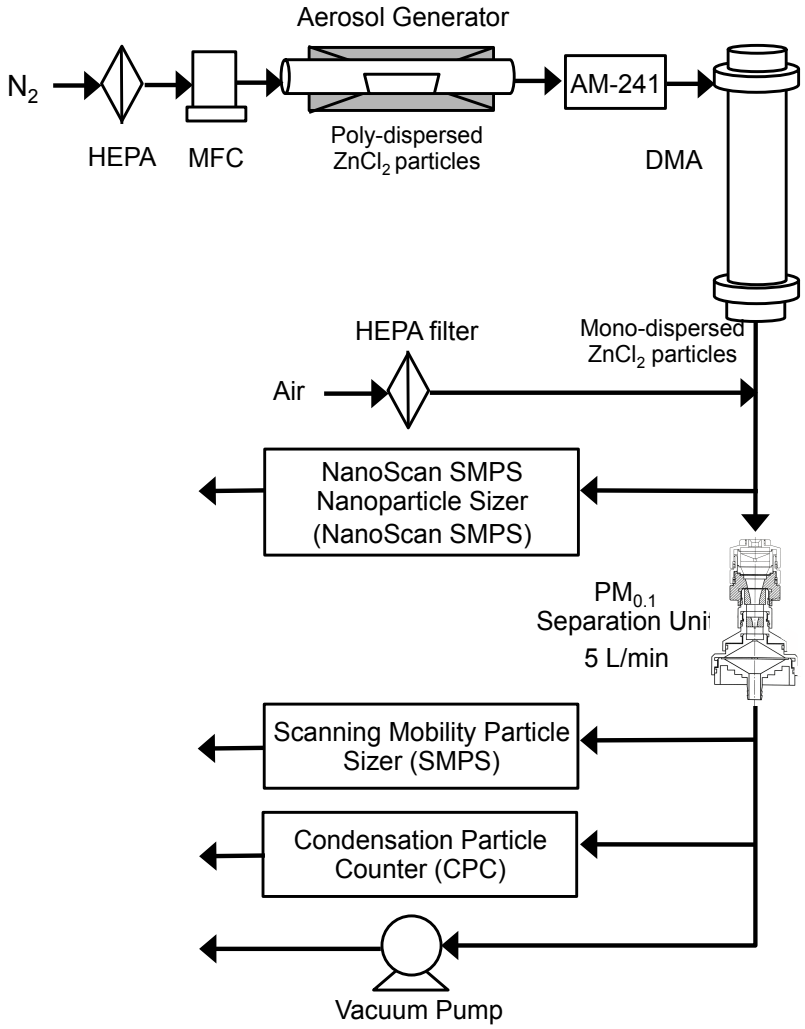

Fig. 4.4 Experimental setup for validation of $PM_{0.1}$ online monitoring system.

4.4.2 Application of the present system for the monitoring of ambient aerosol nanoparticles

As an application of the $PM_{0.1}$ online monitoring system, it was used for the online monitoring of the number concentration of ambient $PM_{0.1}$ particles and associated total black carbon. The configuration of the system is shown in Fig. 4.5.

The ambient $PM_{0.1}$ number concentration and black carbon concentration were evaluated by CPC and MAAP downstream the $PM_{0.1}$ separation unit. In order to determine $PM_{0.1}$ particle mass concentration, SMPS was also located downstream the $PM_{0.1}$ separation unit along with $PM_{0.1}$ sampling by using $PM_{0.1}$ personal sampler to confirm the reliability of the monitoring system. While the NanoScan SMPS and CPC was located upstream the $PM_{0.1}$

separation unit to measure particle number concentration in TSP and 10-470 nm particles to compare with $PM_{0.1}$ number concentration measuring by the CPC. To evaluate the BC in TSP, black carbon monitor (BCM) was located upstream the $PM_{0.1}$ separation unit during MAAP was used to monitor BC in $PM_{0.1}$ particles. Moreover, the collected PM0.1 particles on a filter of $PM_{0.1}$ personal sampler were analyzed for elemental carbon (EC) mass concentration by thermal method to discuss with BC mass concentration measured by optical method using MAAP.

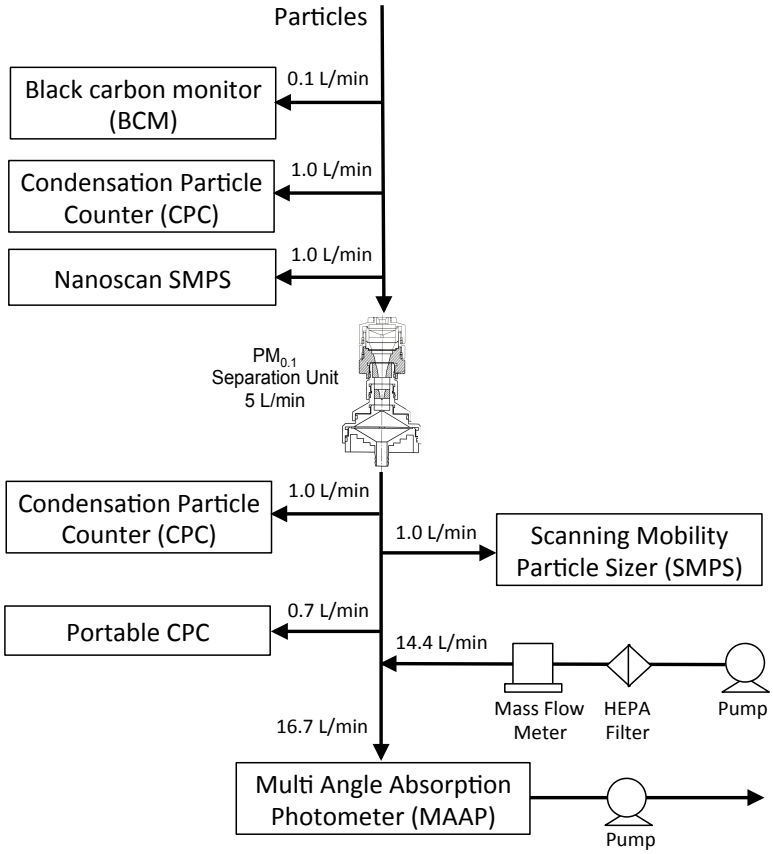

Fig. 4.5 $PM_{0.1}$ and associated BC online monitoring system for ambient particle monitoring

4.5 Results and Discussion

4.5.1 Validation of Concentration of $PM_{0.1}$ using the Present Monitoring System

For validation of the monitoring system, the number concentration of 100 nm mono-dispersed generated $ZnCl_2$ particles were simultaneously measure $PM_{0.1}$ particles by Nanoscan SMPS 3910 upstream the $PM_{0.1}$ separation unit, CPC 3785 and SMPS 3034 downstream the $PM_{0.1}$ separation unit. For the monitoring system, the Nanoscan SMPS, the CPC and the SMPS were found to be a reliable tool to simultaneously monitor $PM_{0.1}$ number

concentration due to similarity of number concentration of 100 nm mono-dispersed generated $ZnCl_2$ particles by a time change as shown in Fig.4.6

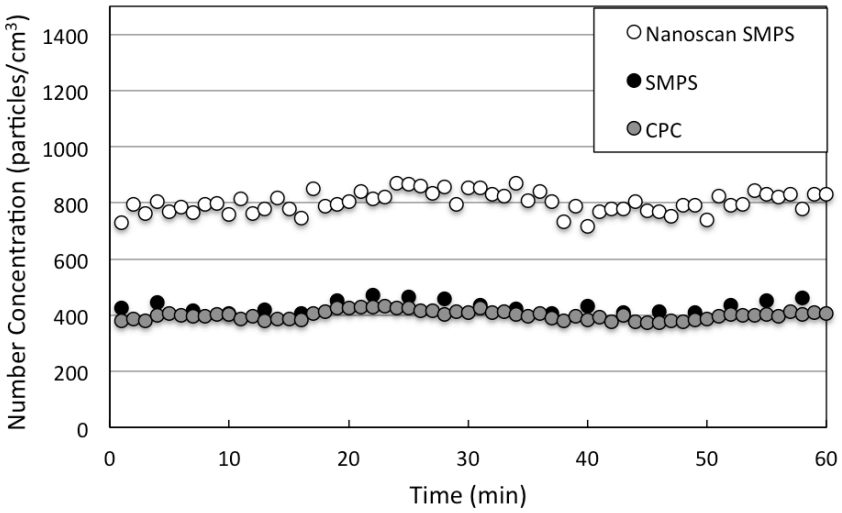

Fig. 4.6 Number concentration of 100 nm mono-dispersed generated $ZnCl_2$ particles obtained by NanoScan SMPS upstream $PM_{0.1}$ separation unit, and SMPS and CPC downstream $PM_{0.1}$ separation unit.

Fig.4.7 shows collection efficiency of $PM_{0.1}$ unit by a time change using mono-disperse generated $ZnCl_2$ particles of 100 nm. The $PM_{0.1}$ inertial filter combined with a pre-cut inertial filter and pre-cut impactors can provide 50% of collection efficiency of 100 nm particles. The $PM_{0.1}$ inlet could be a acceptable practically tool to apply with measuring instruments to monitor $PM_{0.1}$ particle concentration and, or associated chemical compounds.

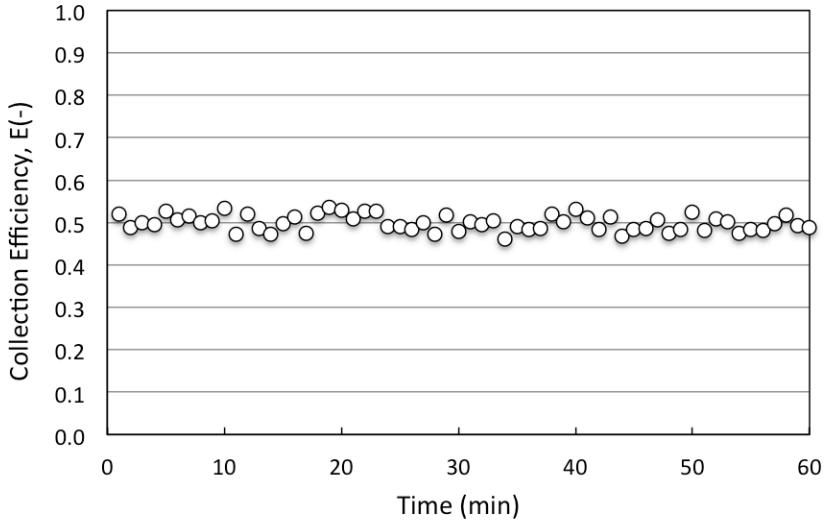

Fig. 4.7 Collection efficiency of inertial filters with pre-cut impactor filters using 100 nm mono-disperse $ZnCl_2$ particles.

4.5.2 Application of the Present Monitoring System to measurement of Ambient $PM_{0.1}$ particles and particle-bound black carbon

Fig. 4.8 shows the number concentration of $PM_{0.1}$ particles measured by CPC3785 and portable CPC 3007, and TSP and 10-470 nm particles measured by CPC3785 and Nanoscan SMPS, respectively. The number concentration of ambient particles showed that the total particles contain $PM_{0.1}$ particles nearly 50%. Fig. 4.9 shows the $PM_{0.1}$ mass concentration measured by SMPS (1.46-3.26 μg/m^3, 2.28 μg/m^3 in average) was similar to the $PM_{0.1}$ mass concentration (2.43 μg/m^3) obtained by the $PM_{0.1}$ personal sampler. The results confirmed that the monitoring of $PM_{0.1}$ particles using the present online monitoring system is reliable.

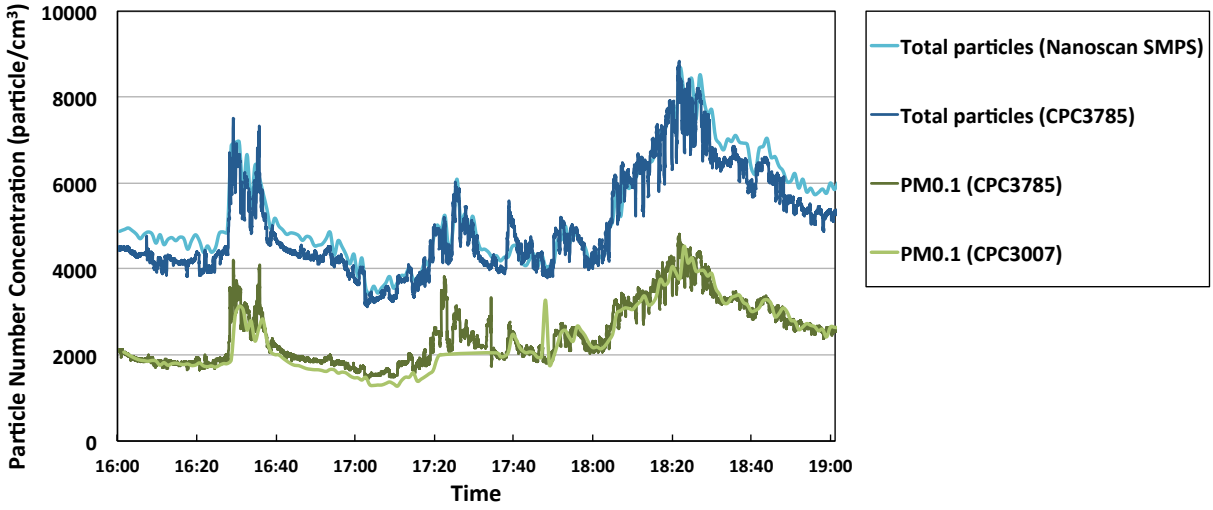

Fig. 4.8 Number concentration of $PM_{0.1}$ and total particles measured by CPC and SMPS.

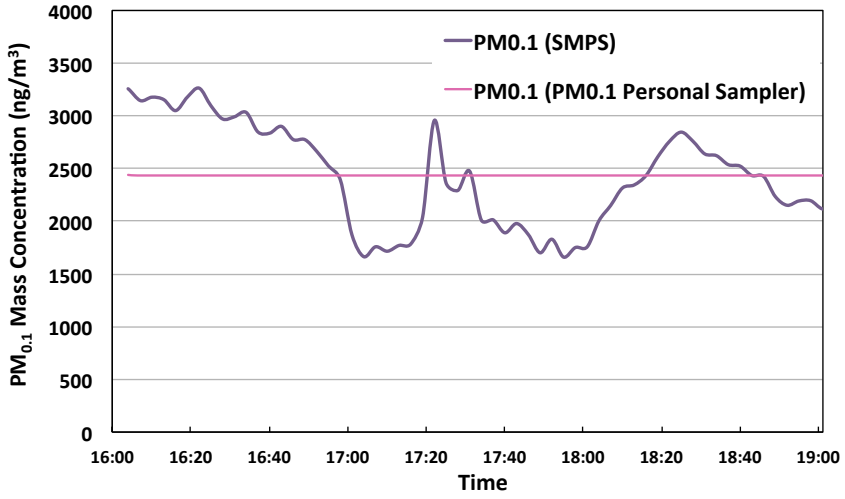

Fig. 4.9 $PM_{0.1}$ mass concentration of $PM_{0.1}$ measured by SMPS and $PM_{0.1}$ personal sampler

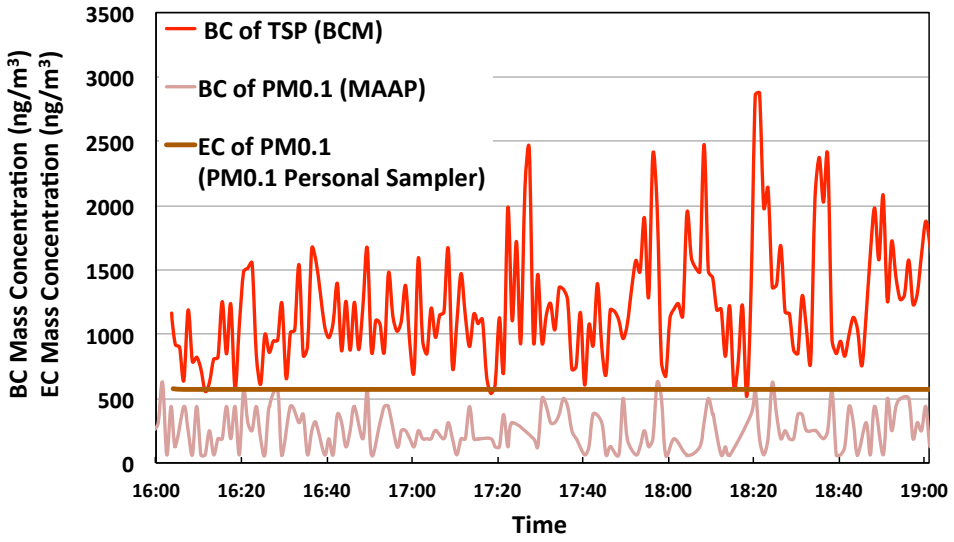

Fig. 4.10 BC and EC mass concentration of ambient particles

Fig. 4.10 shows the BC concentration in $PM_{0.1}$ was ~200 ng/m^3 in average, while the BC concentration in total particles was ~1200 ng/m^3 in average. The fraction of EC in $PM_{0.1}$/BC in $PM_{0.1}$ was 2.22. Therefore, the EC concentration analyzed by the thermal method was higher than the BC concentration measured by the optical method.

Fig. 4.11 shows the calculated $PM_{0.1}$ concentration from Nanoscan SMPS results upstream $PM_{0.1}$ separation unit by collection efficiency of total filters of the $PM_{0.1}$ personal sampler in each particle size, the calculated $PM_{0.1}$ concentration showed similar trend of concentration measured by the CPC (TSI, Model 3785) and the portable CPC (TSI, Model 3007) downstream $PM_{0.1}$ separation unit. The results confirmed that $PM_{0.1}$ separation unit can be used for the online monitoring and a portable CPC can be used to measure $PM_{0.1}$ for the online monitoring system.

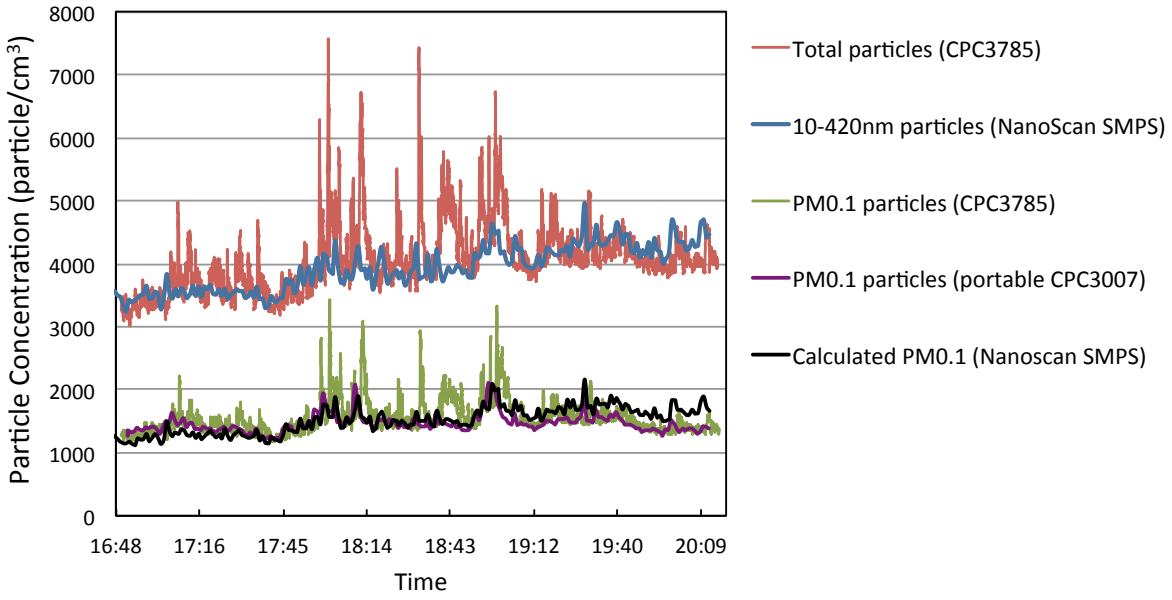

Fig. 4.11 Concentration of measured $PM_{0.1}$ particles, calculated $PM_{0.1}$ particles and measured total particles.

4.6 Conclusion

The $PM_{0.1}$ separation unit, which consists of $PM_{0.1}$ inertial filter for $PM_{0.1}$ separation, the pre-cut inertial filter and pre-cut-impactors for the removal of coarse particles has been successfully applied to the monitoring of the number concentration and black carbon in $PM_{0.1}$ by combining with the condensation particle counter (CPC) both of the CPC model 3785 and the portable CPC Model 3007, and the multi angle absorption photometer (MAAP). The validation of the system confirmed that $PM_{0.1}$ separation unit can be used for the online monitoring for measurement both of $PM_{0.1}$ and particle bound black carbon.

Chapter 5

Conclusion

The $PM_{0.1}$ personal sampler was successfully devised based on the inertial filter technology by improving a prototype of the personal sampler for the evaluation of personal exposure to nanoparticles (Furuuchi et al., 2010). The inertial filter with the layered mesh geometry demonstrated a separation performance with a cutoff size of 100 nm and a small pressure drop. Through the combination of a layered mesh inertial filter for the $PM_{0.1}$ and pre-cut impactors for the removal of huge or coagulated particles along with a pre-cut inertial filter for the removal of fine particles, the present $PM_{0.1}$ inlet for the personal sampler was practical for the chemical analysis of collected particles. The assessment of personal exposure to nanoparticles and their chemical compounds were found to be important in some living and working environments. Moreover, the inertial filters as a $PM_{0.1}$ separation unit, is a simple and desirable tool for combining with the condensation particle counter (CPC) and the multi angle absorption photometer (MAAP) to the monitoring of the number concentration and black carbon in $PM_{0.1}$ particles.

References

Behera, S.N., Xian, H., Balasubramanian, R. (2014). Human health risk associated with exposure to toxic elements in mainstream and sidestream cigarette smoke. *Science of the Total Environment* 472: 947–956.

Allen, J.O., Mayo, P.R., Hughes, L.S., Salmon, L.G., Cass, G.R. (2001). Emissions of size-segregated aerosols from on-road vehicles in the Caldecott tunnel. *Environmental Science and Technology* 35: 4189-4197.

Bolch, W.E., Farfán, E.B, Huh, C., Huston, T.E., Bolch, W.E. (2001). Influence of parameter uncertainties within the ICRP 66 respiratory tract model: Particle Deposition. Health Phys. 81: 378–394.

Borgini, A., Tittarelli, A., Ricci, C., Bertoldi, M., Saeger, E.D., Crosignani P. (2011). Personal exposure to $PM_{2.5}$ among high-school students in Milan and background measurements: The EuroLifeNet study. *Atmospheric Environment* 45: 4147-4151.

Borm, P. J. A., Kreyling, W. (2004). Toxicological hazards of inhaled nanoparticles-potential implications for drug delivery. *Journal of Nanoscience and Nanotechnology* 4(5): 521–531.

Chang, L.T., Sarnat, J., Wolfson, J.M., Rojas-Bracho, L., Suh, H.H., Koutrakis, P. (1999). Development of a personal multi- pollutant exposure sampler for particulate matter and criteria gases. In: Pollution Atmospherique, Numero Special 40 Anniversaire de L'APPA: 31–39.

Choosong, T., 2009. Assessment of working environment and worker's exposure to ultrafine particles and polycyclic aromatic hydrocarbons (PAHs) from biomass wood burning. Ph.D. dissertation. Kanazawa University.

Choosong, T., Chomanee, J., Tekasakul, P., Tekasakul, S., Otani, Y., Hata, M., Furuuchi, M. (2010). Workplace Environment and Personal Exposure of PM and PAHs to Workers in Natural Rubber Sheet Factories Contaminated by Wood Burning Smoke. *Aerosol and Air Qual. Res*., 8–21.

Davidson, C. I., Phalen, R. F., Solomon, P. A. (2005). Airborne particulate matter and human health: A review. *Aerosol Science and Technology* 39(8): 737–749.

Donaldson, K., Brown, D., Clouter, A., Duffin, R., MacNee, W., Renwick, L., Tran, L., Stone, V. (2002). The pulmonary toxicology of ultrafine particles. Journal of Aerosol Medicine : *The Official Journal of the International Society for Aerosols in Medicine* 15(2): 213–20.

Du, X., Kong, Q., Ge, W., Zhang, S., Fu, L. (2010). Characterization of personal exposure concentration of fine particles for adults and children exposed to high ambient concentrations in Beijing, China. Journal of Environmental Sciences 22(11): 1757–1764.

Eryu, K., Seto, T., Mizukami, Y., Nagura, M., Furuuchi, M., Tajima, N., Kato, T., Ehara, K., Otani, Y. (2009). Design of inertial filter for classification of $PM_{0.1}$. *J Aerosol Res*. 24, 24-29 (in Japanese).

Furuuchi, M., Choosong, T., Hata, M., Otani, Y., Tekasakul, P., Takizawa, M., Nagura, M. (2010). Development of a personal sampler for evaluating exposure to ultrafine particles. *Aerosol and Air Qual. Res.* 10: 30–37.

Goossens, D. and Buck, B. (2009). Dust Emission by off- road Driving: Experiments on 17 Arid Soil Types, Nevada, USA. *Geomorphology* 107: 118–138.

Granum, B., Lovik, M. (2002). The effect of particles on allergic immune responses. *Toxicological Sciences : An Official Journal of the Society of Toxicology* 65(1): 7–17.

Hata, M., Zhang, T., Bao, L., Otani, Y., Bai, Y., Furuuchi, M. (2013) (a), Characteristics of the Nanoparticles in a Road Tunnel, *Aerosol and Air Quality Research*, 13: 194–200.

Herner, J. D., Aw,, J., Gao,, O., Chang,, D. P., Kleeman, M. J. (2005). Size and composition distribution of airborne particulate matter in Northern California: I-particulate mass, carbon, and water-soluble ions. *Journal of the Air & Waste Management Association* 55(1): 30–51.

Hinds, W. C. (1999). Aerosol Technology (2nd Ed.). Wiley-Interscience, New York.

Hussain, M., Madl, P., Khan, A. (2011). Lung deposition predictions of airborne particles and the emergence of contemporary diseases Part-I. *the Health* 2(2): 51-59.

IPCC (Intergovernmental Panel on Climate Change, Climate Change). (2007), The Physical Science Basis: Contribution of Working Group I to the Fourth Assessment Report of the Intergovernmental Panel on Climate Change, Cambridge University Press, Cambridge.

Jahn, H.J., Kraemer, A., Chen, X.C., Chan, C.Y., Engling, G., Ward, T.J. (2013), Ambient and personal PM2.5 exposure assessment in the Chinese megacity of Guangzhou, *Atmospheric Environment*, 74: 402-411.

Johannesson, S., Gustafson, P., Molnar, P., Barregard, L., Sallsten, G. (2007). Expo- sure to fine particles (PM2.5 and PM1) and black smoke in the general population: personal, indoor, and outdoor levels. *J. Expo. Sci. Environ. Epidemiol*. 17: 613-624.

Kiurski, J.S., Marić, B.B., Aksentijević, S.M., Oros, I.B., Kecić, V.S. and Kovačević, I.M. (2013), Indoor air quality investigation from screen printing industry, *Renewable and Sustainable Energy Reviews*, 28: 224–231.

Kobayashi, H., Kanoh, S., Motoyoshi, K., Aida, S. (2004), Diffuse lung disease caused by cotton fibre inhalation but distinct from byssinosis, *Thorax*, 59: 1095–1097.

Kuhlbusch, T. A., Asbach, C., Fissan, H., Göhler, D., Stintz, M. (2011). Nanoparticle exposure at nanotechnology workplaces: a review. *Particle and Fibre Toxicology* 8(1): 22.

Lachenmyer, C. (2000). Urban measurements of outdooreindoor PM2.5 concentra- tions and personal exposure in the deep south. Part I. Pilot study of mass concentrations for nonsmoking subjects. *Aerosol Sci. Technol*. 32: 34-51

Lim, S., Kim, J., Kim, T., Lee, K., Yang, W., Jun, S., Yu, S. (2012). Personal exposures to $PM_{2.5}$ and their relationships with microenvironmental concentrations. *Atmospheric Environment* 47: 407-412.

Morawska, L., Ristovski, Z., Jayaratne, E.R., Keogh, D.U., Ling, X. (2008). Ambient nano and ultrafine particles from motor vehicle emissions: Characteristics, ambient processing and implications on human exposure. *Atmospheric Environment* 42: 8113–8138.

Moreland, A. Kijsirichareanchai, K., Alalawi, R., Nugent, K. (2011), Pulmonary alveolar proteinosis in a man with prolonged cotton dust exposure, *Respiratory Medicine CME*, 4: 121-123.

Nicholson, K.W. (1993). Wind Tunnel Experiments on the Resuspension of Particulate Material. *Atmos. Environ.* 27: 181–188.

Ngo, M. A., Pinkerton, K. E., Freeland, S., Geller, M., Ham, W., Cliff, S.,Hopkins, L. E., Kleeman, M. J., Kodavanti, U. P., Meharg, E., Plummer, L., Recendez, J. J., Schenker, M. B., Sioutas, C., Smiley-Jewell, S., Hass, C., Gutstein, J., Wexler, A. S. (2010). Airborne particles in the San Joaquin Valley may affect human health. *California Agriculture* 64(1): 12–16.

Oglesby, L., Kunzli, N., Roosli, M., Braun-Fahrlander, C., Mathys, P., Stern, W., Jantunen, M., Kousa, A. (2000). Validity of ambient levels of fine particles as surrogate for personal exposure to outdoor air pollution e results of the Eu- ropean EXPOLIS-EAS Study (Swiss Center Basel). J. *Air Waste Manag. Assoc.* 50: 1251-1261.

Otani, Y., Eryu, K., Furuuchi, M., Tajima, N., Tekasakul, P. (2007). Inertial classification of nanoparticles with fibrous filters. *Aerosol Air Qual Res* 7: 343-352.

Phillips, K., Bentley, M.C. (2001). Seasonal assessment of environmental tobacco smoke and respirable suspended particle exposures for nonsmokers in Bremen using personal monitoring. *Environment International* 27: 69-85.

Salako, G. O. (2012). Exploring the Variation between EC and BC in a Variety of Locations. *Aerosol and Air Quality Research*, 1–7.

Schauer, J. J., Kleeman, M. J., Cass, G. R., and Simoneit, B. R. T. (1999). Measurement of Emissions from Air Pollution Sources. 2. C1 through C30 Organic Compounds from Medium Duty Diesel Trucks. *Environ. Sci.Technol.* 33:1578–1587.

Schauer, J. J., Kleeman, M. J., Cass, G. R., and Simoneit, B. R. T. (2002). Measurement of Emissions from Air Pollution Sources. 5. C-1-C-32 Organic Compounds from Gasoline-Powered Motor Vehicles. *Environ. Sci. Technol*. 36:1169–1180.

Sehmel, G.A., Hopke, P.K., Cohen, D.D., Begum, B.A., Biswas, S.K., Pandit, G.G., Chung, Y.-S., Rahman, S.A., Hamzah, M.S., Markwitz, A., Shagjjamba, D., Lodoysamba, S., Wimolwattanapun, and Bunprepob, S. (1980). Particle Resuspension: A Review. *Environ. Int.* 4: 107–127.

Seinfeld, J.H. 1975. Air pollution: physical and chemical fundamentals. McGraw-Hill. United States of America.

Takebayashi, M. (2012). Development of an inertial classifier of nanoparticles for real time nano-particle counter. Master degree thesis. Kanazawa University (in Japanese).

Tsai, C.J., Liu, C.N., Hung, S.M., Chen, S.C., Uang, S.N., Cheng, Y.S., Zhou, Y. (2012). Novel active personal nanoparticle sampler for the exposure assessment of nanoparticles in workplaces. *Environmental Science & Technology* 46(8): 4546–4552.

Wallace, L. (1996). Indoorparticles: a review.J. *Air Waste Manag.Assoc*.46: 98-126.

Warheit, D.B. (2004), Nanoparticles: Heath impacts. Materials Today 7(2): 32–35.

Ward, D.J., Ayres, J.G. (2004). Particulate air pollution and panel studies in children: a systematic review. *Occupational and Environmental Medicine* 61: 1-12.

Wilson, W.E., Brauer, M. (2006). Estimation of ambient and non-ambient compo- nents of particulate matter exposure from a personal monitoring panel study. J. Expo. Sci. Environ. *Epidemiol*. 16: 264-274.

Young, L.-H., Lin, Y.-H., Lin, T.-H., Tsai, P.-J., Wang, Y-F., Hung, S.-M., Tsai, C.-J., Chen, C.-W. (2013). Field application of a newly developed personal nanoparticle sampler to selected metalworking operations. *Aerosol and Air Quality Research* 13: 849–861.

Acknowledgement

First of all, I would like to express the deepest appreciation to my advisor, Prof. Dr. Furuuchi Masami, who giving me many opportunities in Japan. Thank you for kind invitation, motivation, valuable discussion, guidance and support.

I would like to express my deepest gratitude to Assoc.Prof. Dr. Mitsuhiko Hata for your great suggestions, guidance and support during my Ph.D. period.

I would like to thank Japanese Government for financial support, Monbukagakusho Scholarship through my Ph.D. study, and The Japan Society for the Promotion of Science (JSPS), The Smoking Research Foundation, and the Environment Research and Technology Development Fund of the Ministry of the Environment, Japan for the financial support on my research.

I would like to thank you all members of Laboratory of Atmospheric Environment and Pollution Control Engineering, Kanazawa University, and my Thai friends in Kanazawa for their kind help and encouragement.

Finally, I would like to express my special gratitude to my family. Thank you.

July 2014

Thunyapat Thongyen